Proceedings of the Indian National Science Academy (2025) 91:971–997
https://doi.org/10.1007/s43538-025-00393-3

RESEARCH PAPER

Fluvio-hydrological drivers largely control the morphology and stability of channel bars in the transboundary Himalayan River Jaldhaka

Biswajit Bera[1] · Sudipa Sarkar[1]

Received: 16 October 2024 / Accepted: 14 January 2025 / Published online: 27 January 2025

Abstract

This present study focused on the spatiotemporal morphological dynamics and stability of channel bars of a tropical braided River Jaldhaka. Eleven sub-reaches, ten randomly selected individual channel bars and nine cross sections across three bars with the channel of Jaldhaka River were studied for the morphological characteristics and stability assessment. A set of channel geometry parameters (length, width, perimeters, bar area, and depth) was considered for the estimation of channel behaviour and several suitable braiding indices were calculated for the understanding of braiding intensity using geospatial datasets (1980–2023). Grain size analysis of eleven samples has been executed for the evaluation of sediment characteristics in bar morphology. Higher Sinuosity Index (*SI*) values in the lower sub-reaches (*SRs*) and lower *SI* near the sub-reaches of the Piedmont zone have been found due to changing channel gradients. The results focused on the lower Braiding Index (*BI*) in the SR-11 at Kurigram of Bangladesh whereas, the bars of this sub-reach are less vegetated than other sub-reaches and non-cohesive (higher proportion of sand and silt) banks and materials are responsible for the dynamicity of channel bars. B8, B9, and B10 indicated the highly dynamic but B1, B3, and B6 are more stable channel bars in terms of changing length, area, width, and perimeters out of ten bars over the studied period. Variability in channel gradient in the upper sub-reaches, changing patterns of fluvio-hydrological configurations, land use, presence of vegetation, rainfall intensity, occurrences of floods, etc. are major factors of bar dynamics and stability over time.

Keywords Bar morphology · Jaldhaka River · Braided channel · Himalayan Foreland Basin (HFB)

Introduction

The nature of braided river channels reflects incessant channel planform shifting (Akhter et al. 2019; Sarkar and Bera 2024), development of steady and unsteady channel bars and islands (Hooke and Yorke 2011; Ghosh et al. 2023c), fast thalweg line migration (Ghosh and Bera 2022), low sinuosity, low longitudinal gradient and high width-depth ratio (Leopold and Wolman 1957). Numerous parameters like bank-full discharge, high velocity, devastating floods, riparian vegetation, high bed shear stress, rainfall, and specific sediment yield from catchment areas control the dynamics of braided river planforms (Howard 1998; Germanoski and Schumm 1993; Egozi and Ashmore 2008). Channel bars are generally topographical higher channel bedforms that are formed by aggradations of river-carried materials such as; sand, silt, clay, pebble, gravel, boulders etc. (Yang and Ouchi 2012; Bera et al. 2022). Usually, the braided channel oscillates laterally within the channel belt by the spatiotemporal fluvio-hydrological drivers (Ghosh et al. 2023a, b, c, d, e).The intensity of braiding varies due to the significant variation in channel discharge, velocity, sediment flux, etc. (Charlton 2007). A significant drop in hydraulic gradient and energy of the stream makes the formation of multiple channels with bars and ultimately, the river channel converts into braided, anastomosing, and anabranching channel patterns within the river corridor (Ghosh et al. 2023d). Channel bed topography also depends on the geological setup, lithology, slope, bed particle size, and valley confinement (Mueller and Pitlick 2013). Occurrences of catastrophic flood events can cause channel bifurcation,

✉ Sudipa Sarkar
sarkarsudipa56@gmail.com

[1] Advanced Geomorphology and Hydrology Laboratory, Department of Geography, Sidho-Kanho-Birsha University, Ranchi Road, Purulia 723104, India

modification of bars and islands, and formation of meander cutoffs (Micheli and Larsen 2011; Ghosh et al. 2023d) on the flood plain. Different shapes of channel bars are the most common feature that develops under different climatic, geomorphic, and hydrological conditions. Generally, the channel thalweg line follows the perennial flow path and other seasonally wet flow paths. River channels with steady bars try to adjust through dynamic lateral and vertical erosion-accretion processes and channel bar bars can be stabilized by the influence of vegetation cover, cohesiveness and fine grain size of bed material and human intervention within the river corridor (Leopold and Wolman 1957; Miall 1987; Charlton 2007; Ashmore 2013; Ghosh et al.2024; Sarkar et al. 2023).

Different channel bars significantly dominate in the braided river such as unit bars and compound bars (Smith 1974). Based on their morphology, unit bars are classified into transverse, longitudinal, diagonal, and point bars (Church and Jones 1982), while compound bars are identified as lateral and lingoid bars (Robert 2003). Numerous studies have categorized bars into different types like forced bars (controlled by physical factors), free bars (developed without any force), and steady and unstable bars (Zolezzi and Seminara 2001). The shape and size of bars can vary under the condition of high and low flow conditions. Meanwhile, submerged bars (known as shoals) grow up during low flow velocity conditions. Similarly, mid-channel bars and braid bars develop across the wider section of the river, whereas lateral bars expand tangentially within the channel. Duro et al. (2015) introduced hybrid bars that develop under different morphodynamics instability and channel metamorphosis. These principal regulating factors include sediment and fluid supply changes, the interaction between erodible banks with fluid flow mechanisms (Dey and Ali 2020), construction of hard and soft river engineering, the influence of tide and waves, and other external controls.

Significant studies focused on the control of vegetation in bar stabilization, human regulation in braided rivers, the impact of channelization on channel morphology, large flood controls on large braided rivers etc. (Yang and Ouchi 2012; Ashmore 2013; Ghosh et al. 2023c). Drainage congestion due to longitudinal and cross-sectional river engineering work regulates the growth of bars and islands and the alteration of channel width and longitudinal connectivity (Miall 1977; Church and Jones 1982; Ashworth 1996; Yang and Ouchi 2012; Ashmore 2013; Akhter et al.2019). Hence, a study has predicted the future channel bar growth by applying an autoregressive model (Saha et al. 2022).

Advancement of Geographic Information System (GIS) and remote sensing techniques become very decisive in comprehending the morphodynamics of channel bars that are globally used for river bank line extraction, river bar area identification, active and non-perennial channel identification, spatiotemporal variation of river accretion-erosion area calculation etc. (Nardi and Rinaldi 2015). To study the channel morphology, different types of channel and braiding indices (Braiding Index (BI), channel sinuosity, and channel count index) have been applied mostly for the morphological analysis of braided streams (Egozi and Ashmore 2008).

The foremost part of the Himalayan frontal thrust is recognized as the Himalayan Foreland Basin. This low-lying Himalayan Foreland Basin is characterized by the deposition of quaternary (Holocene) sediments. Different types of channel bars and multiple threads of channel splitting and rejoining are common overviews of Himalayan Rivers (Ghosh and Bera 2022; Ghosh et al. 2023a). This area is dominated by north-to-southern flowing rivers which make fertile floodplains. Himalayan-originated rivers carry huge amounts of sediments (bed loads and suspended loads) and accumulate (due to changes in channel gradient) within the Piedmont section of the Himalayas. Varying flow conditions present the shape of the channel bars in a distinct way. Therefore, during the high flow regime, the channel erodes maximum and deposits on the deeper part of the channel. Multiplicity in active and passive flow pathways forms different morphological attributes and dynamic bed forms (Ashmore 2013). In the case of the alluvium river channel, significant growth of channel bars directly and indirectly provokes channel shifting or avulsion during devastating floods (Bera et al. 2019; Chamling et al. 2022) and this populated river corridor faces severe geo-environmental hazards and disasters every recurrent year. This study has great societal significance in the populated Ganga-Brahmaputra-Meghna River system, particularly in India and Bangladesh. There is a lack of intensive work on spatiotemporal bar dynamics in Transboundary Rivers like Jaldhaka. Few hypotheses have been framed through comprehensive literature reviews and after repeated field observations and geospatial study, most hypotheses regarding the regulating factors of bar dynamics have been accepted. This study attempts to explore the reasons for bar growth, the causes of morphological dynamics, and the stability of the Jaldhaka River.

Materials and methods

Study area

The lower part of the Jaldhaka River (a right-bank tributary of the Brahmaputra/Jamuna River) system is a part of the Quaternary (Holocene) sediment-laden Himalayan foreland plain. 260 km long transboundary river (flowing through India-Bhutan-India-Bangladesh) Jaldhaka originated as River Dichu from Kupup (27° 19′ 49.92″ N/88° 50′ 43.96″ E) (Bitang Lake or Elephant Lake) at an elevation of

4400 m in the south-east Sikkim (Gangtok district, Sikkim, India) (Fig. 1). The catchment area of this river falls under the lesser Himalayas from where the river flows southward direction following topographic gradient. In the upstream, the river forms a deep gorge and multiple unpaired terraces at both banks but after crossing the mountain front of the Himalayas, the channel gradient has dropped drastically, so that, the river becomes wider and formulate-threaded channels with bars. The braided planform of the Jaldhaka River carries ample amounts of pebble, cobble, boulder and sediments, particularly during monsoon and it makes various types of channel bars and islands within the middle to lower reaches. The entire basin (the area is 5792 sq.km) is elongated shape and numerous tributaries are connected with mainstream such as Bindu Khola, Jhalong Khola, Jiti, Murti, Diana, Angrabhasa, Mujnai, Sutunga, Dharala, Dolong etc. In the Coochbehar district, this River Jaldhaka is popularly known as Mansai and Singimari but when it enters Bangladesh, it is called 'Dharala'. In this present study, we considered the braided stretch of the Jaldhaka River and subdivided into different sub-reaches based on the morphological homogeneity of the river. The present study area receives about 3000 mm to 6000 mm annual average rainfall in the monsoon season (Chakraborty & Datta 2013). Approximately 2 million people live in the entire basin area of River Jaldhaka as per Census data (Census of India 2011).

Geological and fluvial background of the Jaldhaka basin

The tectonically sensitive Himalayan frontal province is highly complex because of its geological history (orogenic movement with thrusting, folding, faulting, etc.), and landscape evolution (Gansser 1964). This area has a high rate of sediment aggradations due to sudden drops in river channel gradient and topographic change. This landscape also witnesses the combined interactions of tectonic impression and climatic inconsistency. Additionally, the Baikunthapur Formation, Kanchenjunga Gneiss, Buxa Dolomite Formation, Daling Group and

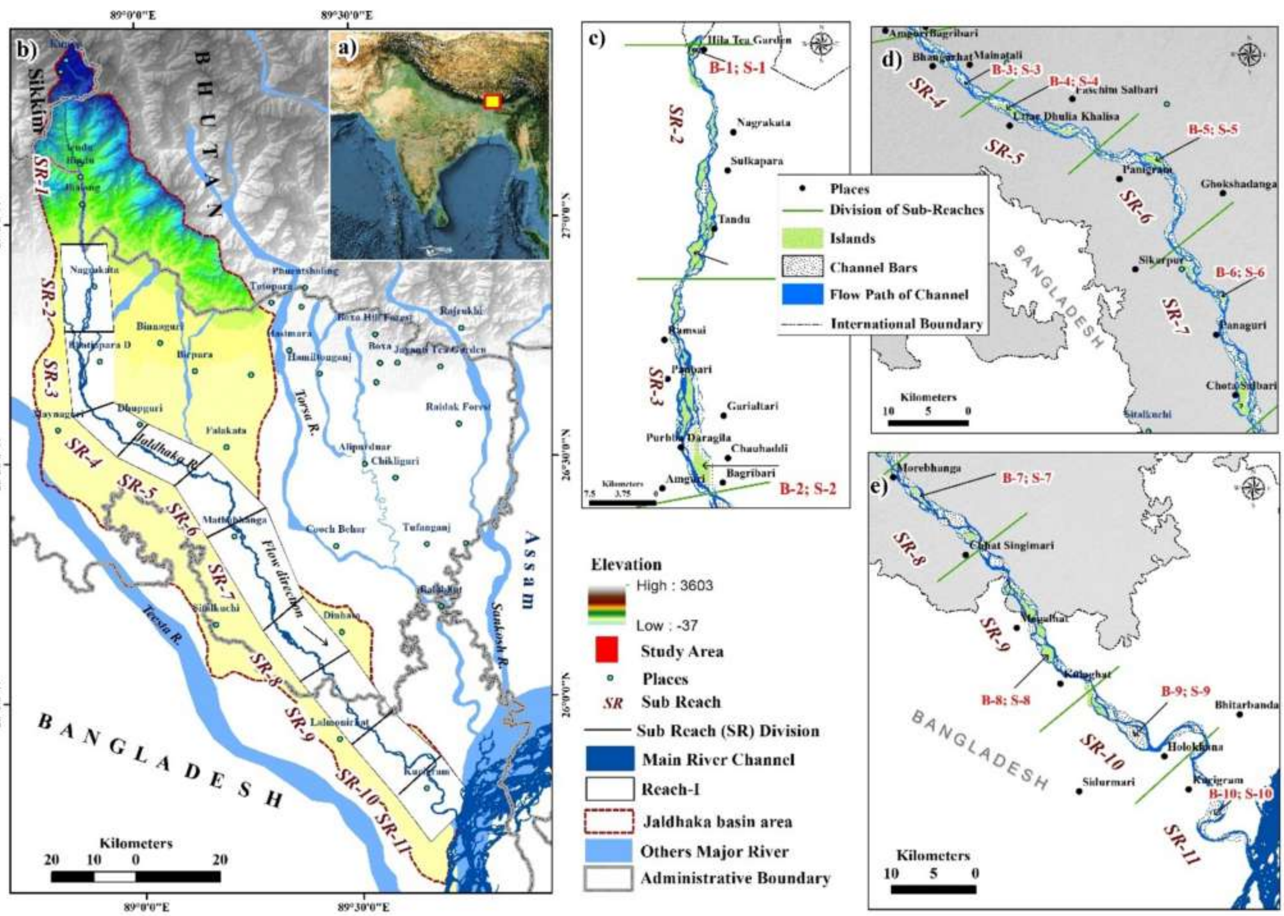

Fig. 1 Location map of the study area. **a** Red box indicates the selected study area, **b** Sub-reaches (SRs) of the Jaldhaka River, **c** Channel bars, islands, and selected sample sites of SR-2 and SR-3, **d** Channel bars, islands, and selected sample sites of SR-4,5,6 and 7, **e** Channel bars, islands and selected sample sites of SR-8,9,10 and 11

Gondwana Super Formation are major geological units that lie beneath the surface (Nakata 1972; Valdiya 1998). In this context, Singh et al. (2016) identified the insights of hydro-geomorphological processes that shaped and deformed the landscape of the Jaldhaka River system geological setup (Fig. 2). The Jaldhaka basin is situated in the active tectonic belt of Eastern Himalaya and foreland area, nearly Himalayan Frontal Thrust (HFT) and Main Boundary Thrust (MBT). This area has diverse range of hydro-geomorphological units such as floodplains, braided streams, riverine depositional features, wetlands etc.

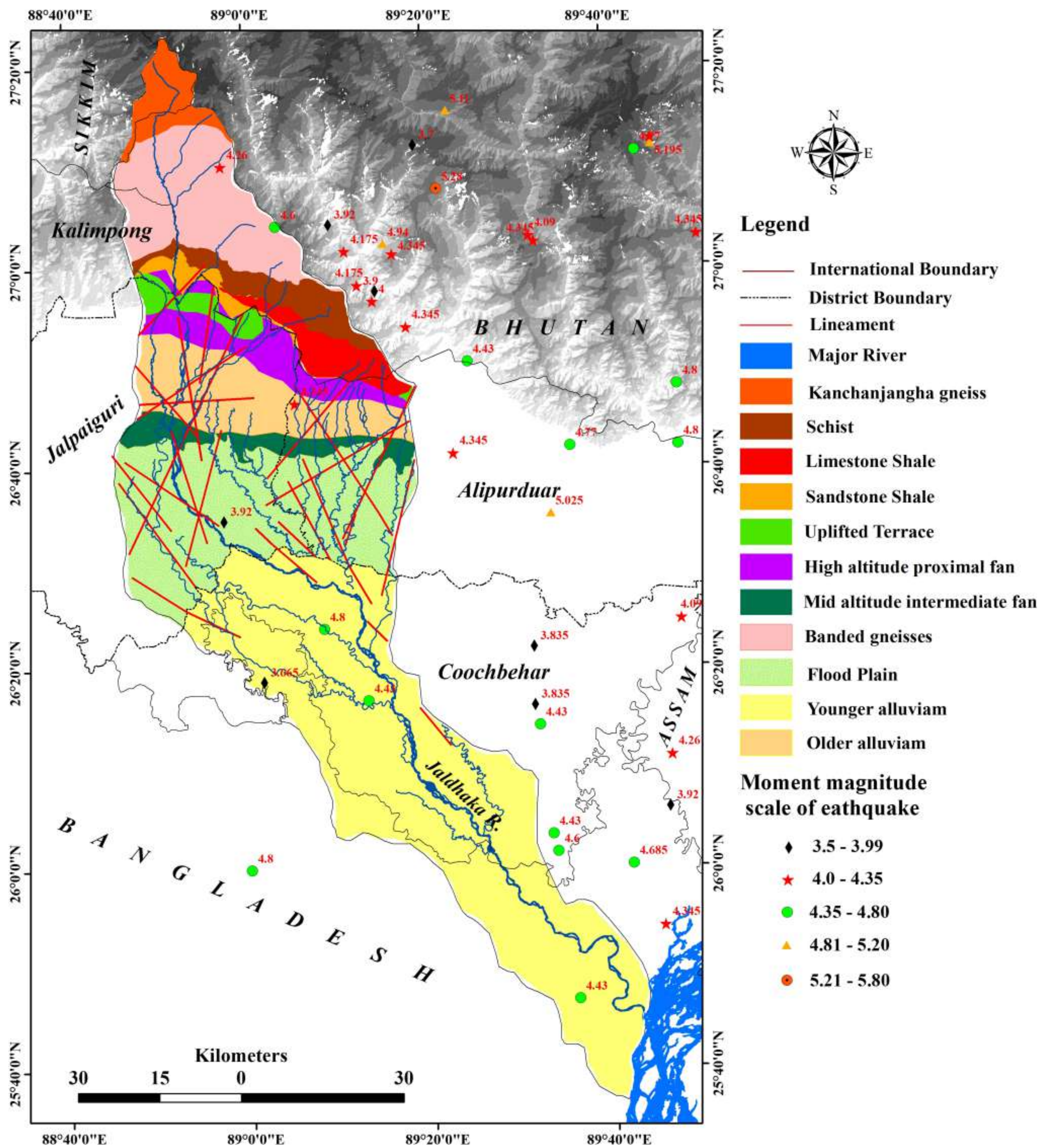

Fig. 2 Geological and fluvial background of the Eastern Himalayan Foreland Basin

Data used and pre-processing

This present study was conducted through extensive field investigation and application of geospatial techniques. Cloud and shadow-free multi-spectral Landsat satellite images have been acquired from the United States Geological Survey (USGS) Earth Explorer (http://earthexplorer.usgs.gov/) and used for the analysis of spatiotemporal dynamics of channel bars of the Jaldhaka river over the last 43 years of time frame. Here, Landsat 1–3 (MSS), Landsat 7 (ETM+) and Landsat 8 (OLI) of the years 1980, 2000 and 2023 have been applied respectively (Table 1). Here, each of the satellite images (raster data) was considered for only post-monsoon season. All the considered satellite images were pre-processed throughout-rectification, radiometric correction and resampled with 30 m spatial resolution. Route Mean Square Error (RMSE) estimation has been done using predicted and observed values of satellite datasets with values of <5 and <0.002 pixels for the geocoding and image registration process. Landsat image-enhancing processes were run through the histogram equalization algorithm of Arc GIS 10.8. Moreover, image mosaicking and stacking were done in the Erdas Imagine (version 14) software. Google Earth images (using Google Earth Pro) have also been used for the recent (2023) river plan view and identification of channel bed features (mainly different types of channel bars and islands).

River course, bar area demarcation and reach-wise spatiotemporal dynamics of channel bar

The most common methods for delineation of water-covered areas and segregation of land–water area of the earth's surface are NDWI and MNDWI. Initially, McFeeters (1996) propounded the algorithm of NDWI which has been widely used for water area demarcation. Later on, Xu (2006) slightly modified the method for better accuracy of water body demarcation, thresholding, noise reduction and sensitivity to water as well as soil moisture. Here, NDWI and MNDWI have been calculated using these robustly used formulae and entire processes were done through the Raster calculator tool of the Arc GIS 10.8 software platform.

$$\mathrm{NDWI} = \frac{Green - NIR}{Green + NIR} \quad (1)$$

Here, NDWI is the Normalized Difference Water Index and NIR means Near Infrared. In this equation, the NIR band has been used only for of Multispectral Scanner (MSS) image.

$$\mathrm{MNDWI} = \frac{Green - SWIR}{Green + SWIR} \quad (2)$$

So, MNDWI stands for Modified Normalized Difference Water Index and SWIR is an abbreviation of Short-Wave Infrared bands. MNDWI has been computed for the delineation of river bank lines from Landsat images (in the case of TM, ETM+ and OLI images).

Furthermore, the channel bar area has been demarcated from raster datasets using a manual digitization tool. Each channel bar of different segments of the river was carefully identified and polygon features. Different morphological attributes such as; total channel area (including bars and islands), total flow path area (excluding bars and islands), channel reach length, bar area, vegetation-covered area, bar width, bar length, the total number of nodes, bar perimeter, number of flow paths within the river etc. have been calculated and measured using Arc GIS software.

Computation of river discharge datasets

Fluvio-hydrological parameters of rivers are very crucial for the study of channel morphodynamics. Hydrological datasets are basic requirements to understand the flow regime, sediment transport, channel migration, channel bar formation and dynamics, occurrence of flood etc. In this concern, the Jaldhaka is a transboundary river, so, hydrological datasets are not available. Here, we considered nine distinct cross-sections across three selected stretches of the Jaldhaka River. The first segment is located near Mukuldanga, while the second

Table 1 Sources of acquired datasets which are used for this study

Types of data	Name of data	Date	Name of sensor	Path/row	Data file format	Spatial resolution (in m)	Source of data
Satellite images (geospatial data)	LANDSAT- 1–5	14-04-1980	MSS	148/042	Tagged image file format (TIFF): georeferenced	60	USGS Earth Explorer (http://earthexplorer.usgs.gov/)
	LANDSAT- 4/5	06-05-2000	TM	148/042		30	
	LANDSAT- 8	14-02-2023	OLI	148/042		30	
Image	Photographs	2022 & 2023	–	–	JPEG	–	Field survey
Image	Google earth images	2023	–	–	JPEG	–	Google Earth Pro software platform
Hydrological data	River discharge	2022	–	–	Excel files	–	Field survey

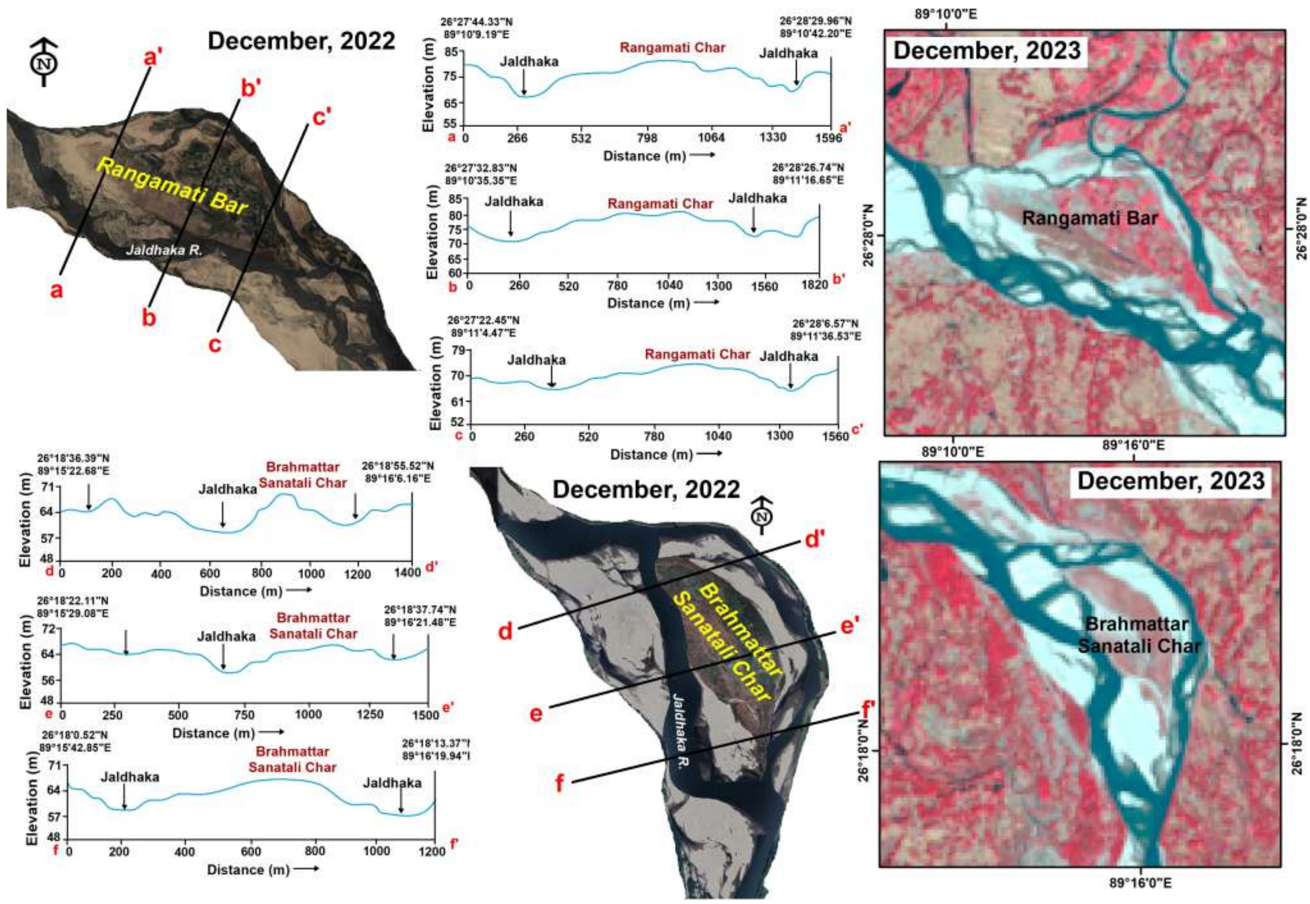

Fig. 3 Cross-sections wise channel profiles of selected channel bars (namely Rangamati bar near Mukuldanga and Brahmattar Sanatali char near Nishiganj) indicated the bed elevation in accordance with channel width (distance)

location is near Nishiganj (Fig. 3) and the third one is located at Adabari Ghat of Singimari (Jaldhaka) River (Fig. 4). Ten days of monsoon and the post-monsoon season were considered during extensive field visits in 2022 and 2023. Flow velocity was measured using a digital current meter and cross-section wise channel depth and width were also measured. Further, the cross-sectional area has been calculated from width and depth datasets. Wetted perimeter, flow top width, and channel slope were also measured. However, discharge data has been estimated by applying the area-velocity method using this formula.

$$Q = A \times V \tag{3}$$

Here, Q represents discharge, A denotes a cross-sectional area and V means channel velocity.

Computation of channel indices

Braiding Index (*BI*)

Channel braiding can be quantified through the calculation of the Braiding Index (BI). Primarily, BI was first calculated by Brice (1964). Further, the Braiding Index has been calculated and modified the formula by numerous scholars such as Rust (1977); Ashmore (1991), Friend and Sinha (1993), Germanoski and Schumm (1993) and Egozi and Ashmore (2008). Here, BI has been calculated for the

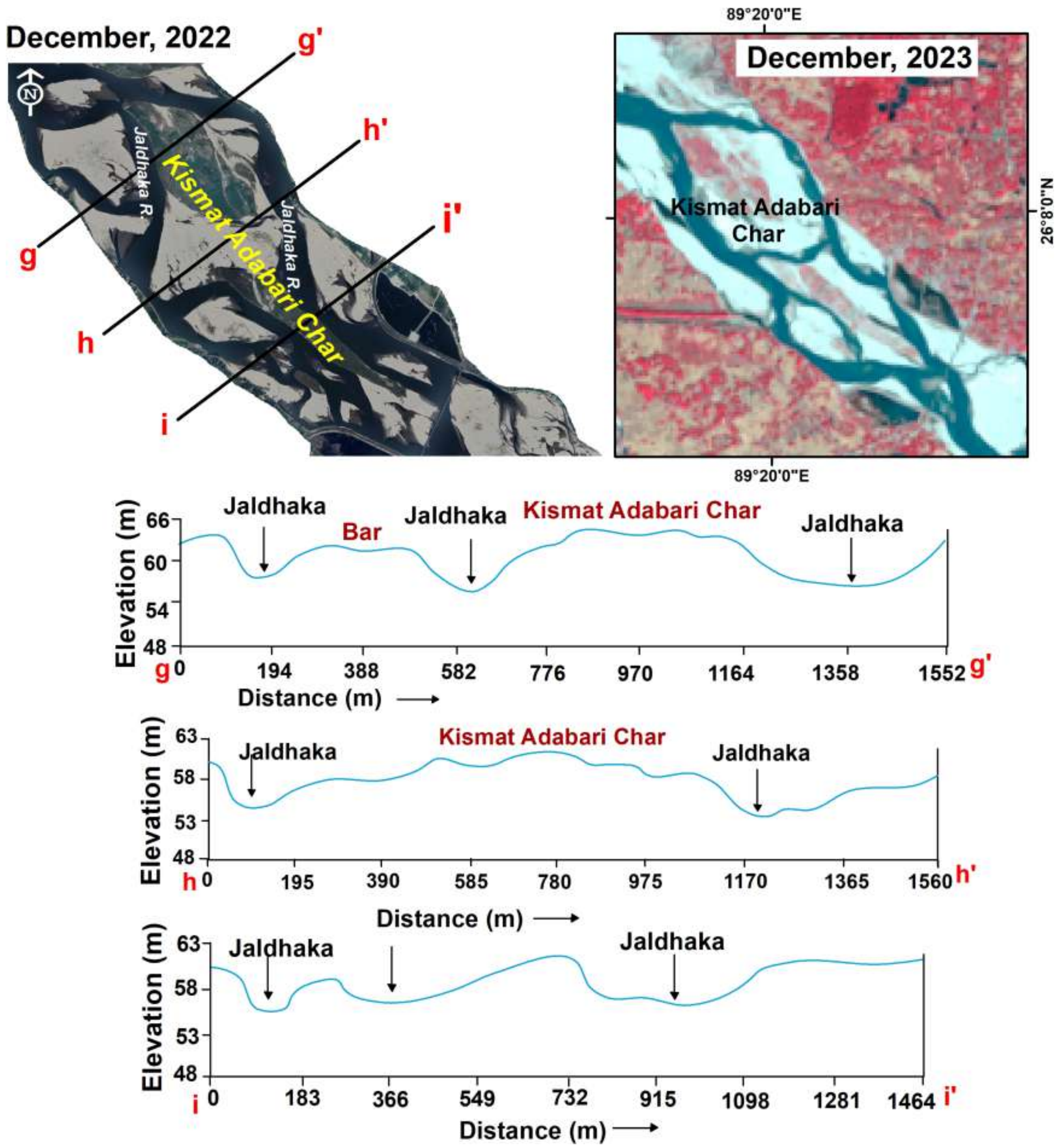

Fig. 4 Cross-sections wise channel profiles of selected channel bars (Kismat Adabari char near Adabari Ghat) indicated the bed elevation in accordance with channel width (distance)

studied sub-reaches of River Jaldhaka using Landsat datasets from 1980 to 2023.

Total Braiding Index (*TBI*)

TBI is one of the important quantitative methods for the measurement of the intensity of braided rivers. The splitting and rejoining of the channel in the braid system indicate the nature of bar formation and its magnitude. Here, flow paths of wetted channels in a considered cross section across the river has been considered for the calculation of TBI.

Channel Sinuosity Index (*SI*) and Total Sinuosity (*SIT*)

The channel sinuosity index has been calculated for eleven sub-reaches of the Jaldhaka River to estimate the deviation of channel curvature from the straight-line flow path. This quantitative measurement was first proposed by Leopold and Wolman (1957). Later on, this index was modified by Schumm (1963), Mueller (1968) and Friend and Sinha (1993). Total sinuosity refers to the ratio of the total length of an individual channel in a reach and the total length of that particular reach in a braided stream.

Plan Form Index (*PFI*)

The Planform Index is a metric formulated by Sharma (2004). It is used to quantify the intensity of the braid bar within the braided channel. The spatiotemporal variation of braided stream can be measured through this index and it can be used for channel classification and evolution of channel through braiding processes as well as making some inferences of braid bar development and erosion.

In this paper, PFI has been calculated for the years 1980, 2000 and 2023 of ten different sub-reaches of Jaldhaka River. Sharma (2004) proposed some threshold values of the Planform Index in braided channels; such as the *PFI* value of a highly braided stream should be $PFI < 4$, *the PFI* value should be between 4 and 19 for a moderately braided stream and when the *PFI* is greater than 19 that indicates low braid stream. Furthermore, numerous studies considered this metric to quantify the braiding behavior of river channels (Akhter et al. 2019

Flow Geometry Index (*FGI*)

The Flow Geometry Index is a measurement of the hydraulic efficiency of a channel. This index stands for the relationship between the width and the depth of the braided channel. The controlling factors of FGI are the channel velocity, settling velocity, bank shear stress etc.

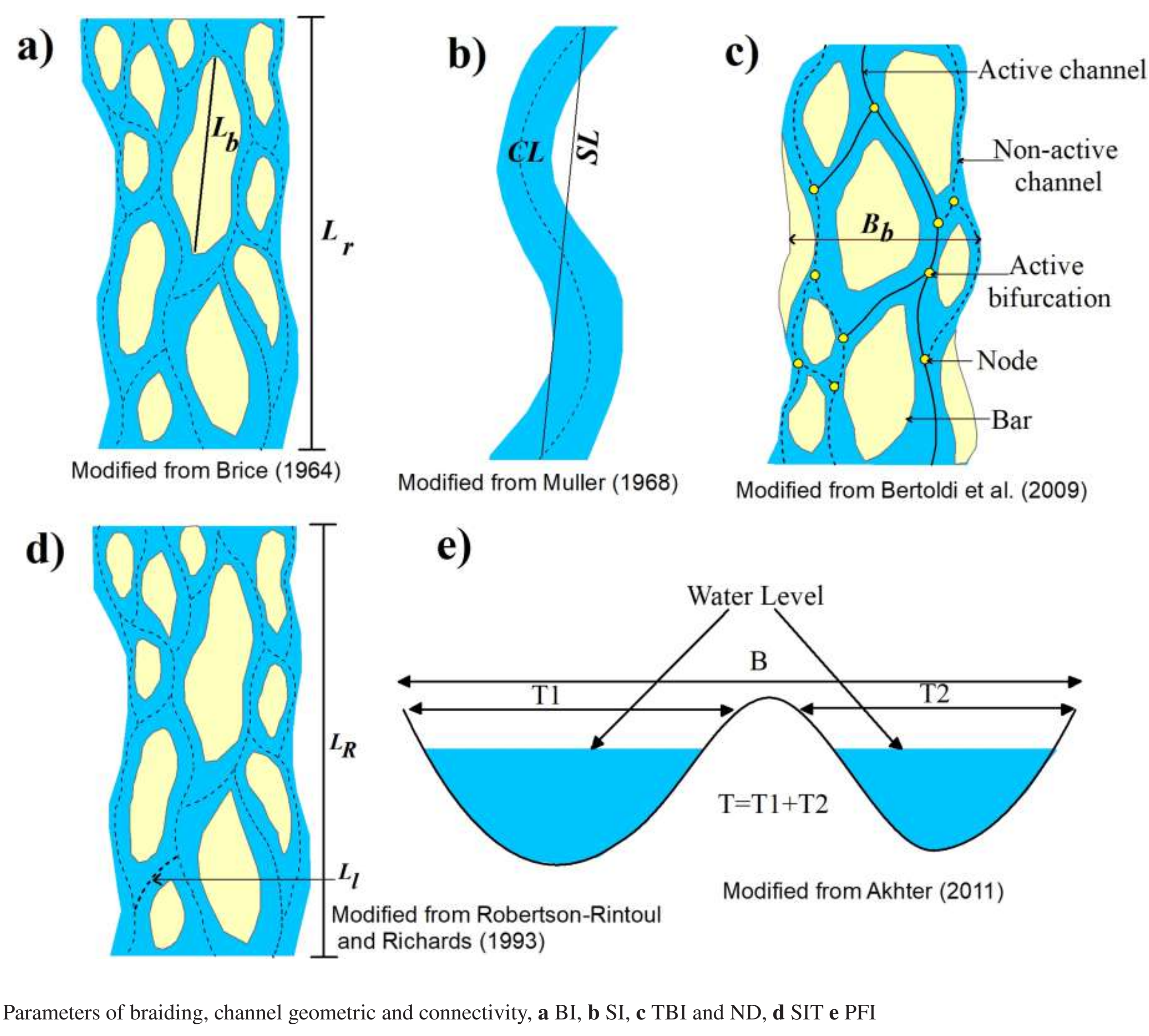

Fig. 5 Parameters of braiding, channel geometric and connectivity, **a** BI, **b** SI, **c** TBI and ND, **d** SIT **e** PFI

Table 2 Derivation of braiding indices; such as *BI*, *TBI*, *SI*, S_{IT}, *PFI*, *FGI* and *ND*

Indices	Equation	Acquired from	Parameters definition
BI	$BI = \frac{2\sum Lb}{Lr}$ (4)	Brice 1964	L_b is length of each channel bar; L_r represents the total length of considered reach (Fig. 5)
TBI	$TBI = Ac/Tw$ (5)	Bertoldi et al. 2009	*Ac* is active channel across the cross section; *Tw is the total width of channel*
SI	$SI = CL/SL$ (6)	Muller1968	*CL* is channel length; *SL* is straight line distance
S_{IT}	$S_{IT}=\sum L_l/L_r$ (7)	Robertson-Rintoul and Richards1993	L_l is length of all channels in the reach; L_r is total length of that particular reach
PFI	$PFI = \frac{\frac{T}{B}\times 100}{N}$ (8)	Sharma 2004	*T* represents flow top width in m which is water surface width of the channel; *B* denotes average width of the channel reach in m and *N* signifies number
FGI	$FGI = \frac{\sum di.Xi.}{W.D} \times N$ (9)	Sharma 2004	Average width (*W*) and depth (*D*) of the channel of each reach has been considered for the calculation of *FGI*. Where, *Di* and *Xi* are the depth and distance of the sub-channel and *N* denotes the number of channels in the sub-reach
ND	$ND = \frac{Nodes}{A} B_b^2$ (10)	Bertoldi et al. 2009	*A* is area; B_b is the bank-to-bank distance across the cross-section

Node Density (*ND*)

Bertoldi et al. (2009) have defined the Node Density of the braided stream for the calculation of several nodes in a unit of channel area. Node density is defined as the number of nodes (Fig. 5) per unit area of the channel, scaled with the belt width to obtain a dimensionless parameter (Table 2).

Sediment sample grain size analysis

Sediment grain size is one of the important aspects of studying the stability of channel bedforms (bar) dynamics. Braided rivers are characterized by various-sized sediments from source to confluence. Channel bed material samples were collected by hand scoop from eleven sub-reaches of Jaldhaka River in the field phase (during post-monsoon (December) season of 2023). Each sample was stored in an air-tight packet and labeled with sub-reach id and place. Initially, unusual debris is removed from the sample and measured each of the samples. Later on, samples were dried to remove the moisture from the soil. The sieve samples were separated into their particle size in different fractions. The samples were sieved separately and carefully measured the weight of every fraction. The percentage was calculated for each sample after repeated sieving of the samples. In the grain size analysis phase, the measured sieve data has been tabulated by the different categories of grain i.e. clay silt, sand, gravel, and pebbles.

Results

In this study, we investigated the spatiotemporal channel bar morphodynamics of the braided river Jaldhaka based on remotely sensed datasets and extensive field investigation.

Reach scale morphodynamics of channel bar

Sub-reach (*SR*) wise morphodynamics (Fig. 6, 7 and 8) variables have been considered for the estimation of channel alteration in response to channel bar modification. Here, sub-reach wise channel length (*CL*), total bar area (*TBA*), total vegetated area in bar (*TVA*), total channel area including and excluding bar (*TCA*), channel flow top width (*T*), width of the channel bank to bank (B_b) and total number of braided channels in the reach (*N*)were calculated for the understanding of channel bar morphodynamics. Results showed that the total length of the SR-2, SR-5, and SR-9 decreased from 1980 to 2023 but SR-11 and Sr-3 showed increased channel length over the study period. Therefore, the total areas of the channel bar (sub-reaches of the upstream) such as SR-3 and SR-4 has been decreased from the year 2000 to 2023. On the other hand, downstream sub-reaches (SR-10 and SR-11) indicated the increasing total bar area from 1980 to 2000 and afterward, the area of bars has been decreased in the year 2023.

In this context, the vegetation cover plays an important role in stabilizing the channel bar and in-stream erosion-accretion dynamics. Here, the total area of vegetation on the bars have been significantly varied over the 43 years. The results indicated that the vegetation-covered area was 6.76 km^2 in 1980 and it reduced in 2000 (3.46 km^2) and further increased to 5.89 km^2 and similarly this type of the result was shown in the SR-3 in between the study period. The total area of the channel bar including vegetation decreased within time (12.32 km^2 in 1980, 9.30 km^2 in 2000 and 8.25 km^2 in 2023) in these sub-reaches. The same decreasing trend is also followed by the SR-3. Consequently, there was no vegetation cover which was found within the channel bar for the SR-10 and SR-11 in the years 2000 and 2023. Furthermore, the average bar areas in the years 1980, 2000 and 2023 were 14.20 km^2, 16.35 km^2 and 14.67 km^2 respectively.

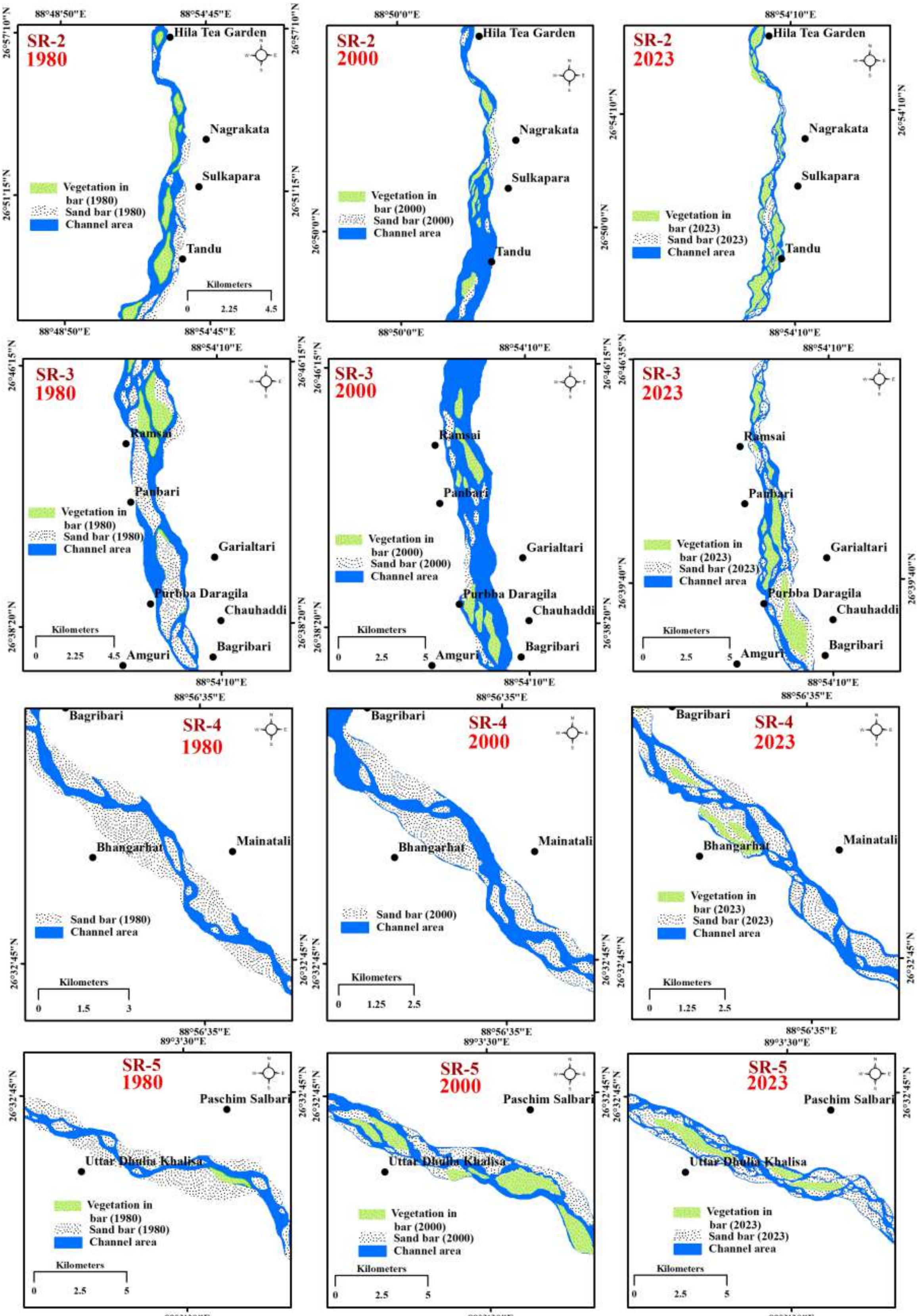

Fig. 6 Spatiotemporal morpho-dynamics of channel bars of SR-2, SR-3, SR-4 andSR-5 in 1980, 2000 and 2023

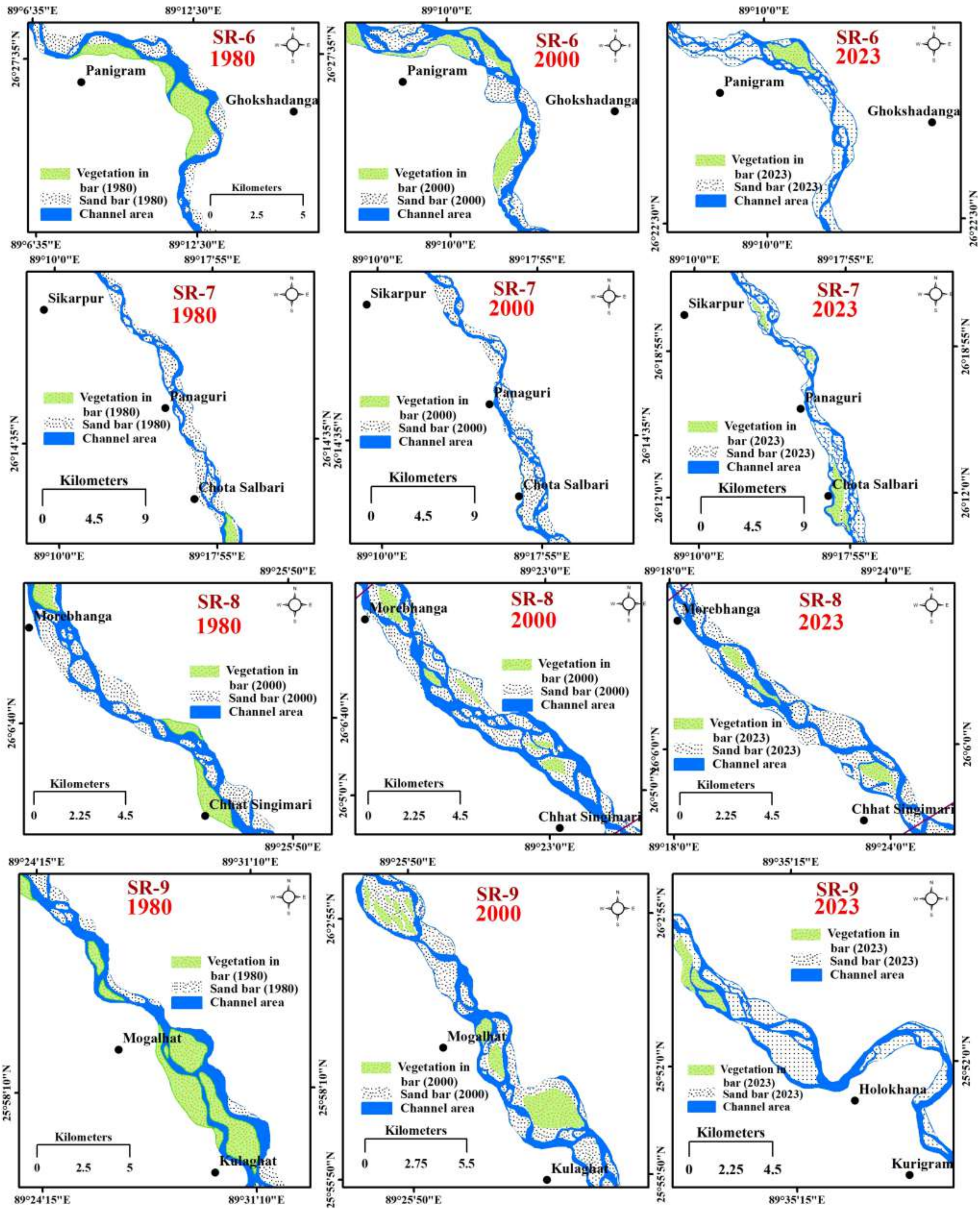

Fig. 7 Spatiotemporal morphodynamics of channel bars of SR-6, SR-7, SR-8 and SR-9 in 1980, 2000, and 2023

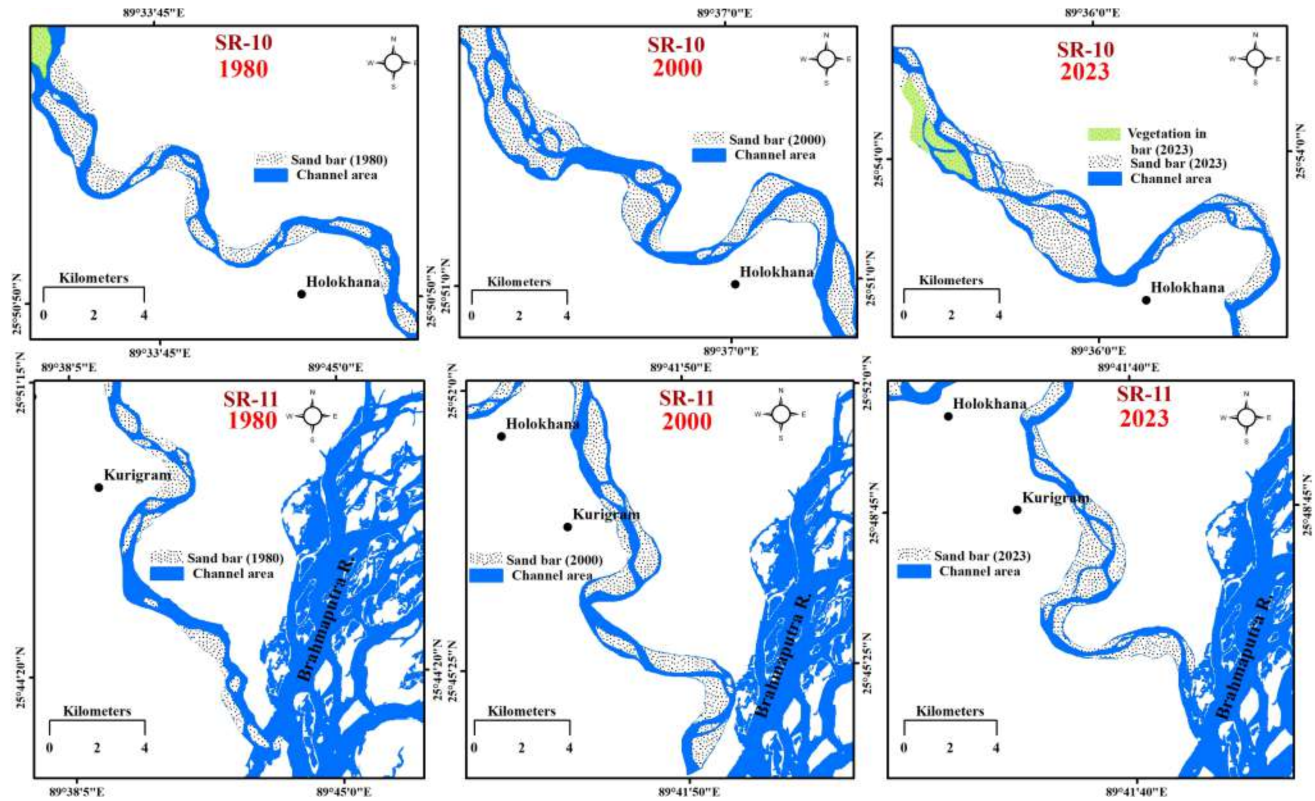

Fig. 8 Spatiotemporal morpho-dynamics of channel bars of SR-10 and SR-11 in 1980, 2000 and 2023

Afterward, the total channel area (including bars) was higher in 1980 for the case of SR-2 and SR-3 but the rest of the sub-reaches were found with higher channel areas in 2000. Further, the decreased value of channel area has been found for these sub-reaches in 2023. However, the Channel area has been reduced (recorded in 2023) in the case of SR-2 and SR-3. These results indicated that the channel narrowing-widening processes are common in between Himalayan foothills and Himalayan foreland basins.

Morphological variation of selected channel bars

Here, ten bars were selected for the analysis of morphological variation particularly in the years 1980, 2000, and 2023 (Fig. 9). Here, results indicated that the length of oval-shaped bar B1 (a mid-channel bar located near Hila tea garden) is increased gradually towards upstream within the studied period, i.e. the length in 1980 was 1.05 km, 1.21 km in 2000 and 1.53 km in 2023 but the width of this bar in 1980 was 0.48 km which decreased in 2000 (0.35 km). Further, it increased in the year 2023 (0.67 km), so the shape of this bar changed from oval to elliptical within the studied period. Similarly, an elongated-shaped point bar is located near Amguri (B2), and it shows a maximum length of 8.28 km (in 1980) and decreased its length gradually in 2000 (6.68 km) and 2023 (5.98 km). Here, the results signify that the width of this bar was 1.31 km in 1980 but it has reduced its width in 2000 (0.29) and further, the increased width was recorded in 2023 (1.51 km). Consequently, decreasing bar length and width of B3 (located near Bhangarhat) and B4 (near Jore Simuli) have been observed from 1980 to 2023. However, a 3.45 km long (2023) irregular shaped channel bar is located near Mukuldanga (B5) which was 2.36 km and 2.05 km long in the year 2000 and 1980 respectively. This bar was previously transverse but presently it has transformed into a complete mid-channel bar and the bar area has increased from 1.36 km^2 (2000) to 2.53 km^2 in 2023. The length and width of the B6 bar (located at Brahmattar Sanatali) were 3.35 km and 1.30 km (triangular shaped) in 1980 but both length and width have decreased in the year 2000 and further increased the value of length–width recorded in 2023 (Table 3). Here, B1 and B3 are comparatively stable out of ten selected bars. On the other hand, areas of B2, B5, B6, B7, and B9 follow the increasing trend of bar area and similarly, B4 and B8 are decreasing in terms of bar area within the study period.

Determination of channel patterns and intensity of braiding

Sub-reach-wise channel and braiding indices were calculated by the spatiotemporal datasets. Here, *SI* (Sinuosity Index) and S_{IT} (Total Sinuosity) have been computed to understand the channel pattern of sub-reaches of this river. The highest sinuosity value was noticed at SR-10 (1.32) in 1980 and the lowest sinuosity measured at SR-3 and SR-4. Similarly, the highest SI value was noticed at SR-11 in 2000 (1.40) and 2023 (1.36) but the lowest SI value was recorded at SR-3 and SR-7 (1.02). SI value ranges from 1.01 to 1.40 within the considering study period of 1980–2023 (43 years).

On the other hand, the results of S_{IT} values are varied from *SI* because here, the entire wetted active channels were considered. The results showed that the highest S_{IT} values shown during the study period in the case of SR-3 (2.31 in 1980, 2.21 in 2000 and 2.09 in 2023) which means the SR-3 was more sinuous among other sub-reaches of river Jaldhaka. Although, SR-1, was not considered during the calculation of S_{IT}.

Braiding Index (*BI*) and Total Braiding Index (*TBI*) have been computed for the ten sub-reaches (SR-2 to Sr-11) of the Jaldhaka River. Previously, Sarkar and Bera (2024) calculated the *BI* of this river for the estimation of braiding intensity. Here, the *BI* value varied between 2.06 and 3.55 over the entire study period. The highest *BI* value (3.55 in 1980, 3.15, and 3.53 in 2023) has been observed in the case of SR-2.

Similarly, the results of *TBI* value vary based on the splitting and rejoining of the active and inactive channels within the corridor of the braided river. Minimal braiding represents low *TBI* and a higher *TBI* value indicates the higher intensity of channel braiding. Here, the *TBI* value ranges from 0.82 (SR-10) to 1.64 (SR-4) in 1980, 0.90 (SR-6) to 2.34 (SR-4) in 2000, and 0.91(SR-6) to 3.13 (SR-5) in 2020 (Table 5).

Plan Form Index (*PFI*) indicates the insights of the channel geometry of braided or meandering channels. Here, *PFI* has been optimized for the years 1980, 2000, and 2023 within ten sub-reaches. *PFI* helps to classify the channel behaviour whereas, lower *PFI* denotes a highly braided channel and higher *PFI* represents the lower braided to the meandering channel. However, a higher *PFI* value was found at SR-5 (30.91), and a lower value was observed at SR-3 (12.50) among ten sub-reaches of the Jaldhaka River. Similarly, the SR-8 and SR-3 showed the highest and lowest *PFI* values in 2000 and SR-6 (31.78) and SR-2 (10.23) also illustrated the highest and lowest value of *PFI* in 2023.

Reach-wise Flow Geometry Index (*FGI*) has been optimized for the ten reaches of the Jaldhaka River. It can be figured out from the results that, the *FGI* value is drastically increased at SR-2 within the study period. On the other side, the SR-3 shows a decreased *FGI* (8.96 in 1980) value in 2000 (5.91) and a further increased value in 2023 (13.27). Moreover, the SR-3 and SR-4 showed a similar decreasing-increasing trend from 1980 to 2023. SR-5, SR-8, SR-9, and SR-10 demonstrated similar increasing trends to SR-2 and SR-6, SR-7, and SR-11 have followed the increasing–decreasing trend of FGI within 43 years.

Finally, Node Density (*ND*) has been calculated to understand the relationship of channel flow path edges and bifurcation points in the braided channel. The highest ND value has been found at the SR-4 in the years 1980 (5.40), 2000 (4.90), and SR-2 (5.25) in 2023. The ND value varies based on the active and inactive flow paths of the channel over time.

Variation in fluvio-hydrological parameters

The spatiotemporal changes of channel bar morphological parameters such as bar length, width, height, perimeter, area etc. can be varied with the fluvio-hydrological control and human intervention in the channel corridor. Here, cross-section average discharge has been computed based on the field datasets for post-monsoonal months (November–December) of 2022 and monsoonal months (July–August) of 2023 (Tables 6, 7). Nine cross-sections have been studied across three randomly selected bars with active and non-active channels of the Jaldhaka River. The result shows the variation in fluvio-hydrological parameters (water level, average velocity, flow top width, wetted perimeter, cross-sectional area, average channel depth, channel discharge, and slope) in recent years (2022 and 2023). Table 6 shows post-monsoonal variation of discharge (ranges between 267.28 to 3.44.25 m^3/s) whereas, the cross-sections a–a′, b–b′, and c–c′ (which are located across the Rangamati bar near Mukuldanga village) have the highest average width-depth ratio (W/D) (1672.10) in the post-monsoonal months of 2022. The flow top width was higher across the cross sections of g–g′ (609 m), h–h′ (633.25 m), and i–i′ (608.30 m) and the wetted perimeter is higher across these three cross-sections (Table 6).

On the other hand, it is observed from the results that, the higher discharge recorded across the cross sections g–g′, h–h′, and i–i′ of the bar (Kismat Adabari char) located at Adabari Ghat of Singimari (Jaldhaka/Mansai) River in the monsoon season of 2023. 1923.38 m^3/s, 2126.51 m^3/s and 2190.40 m^3/s discharge was found across the cross sections of d–d′, e–e′ and f–f′ (across the bar Brahmattar Sanatali) accordingly (Table 7). In monsoonal months higher average width-depth ratio (770.14) was observed across the cross sections of a–a′, b–b′, and c–c′.

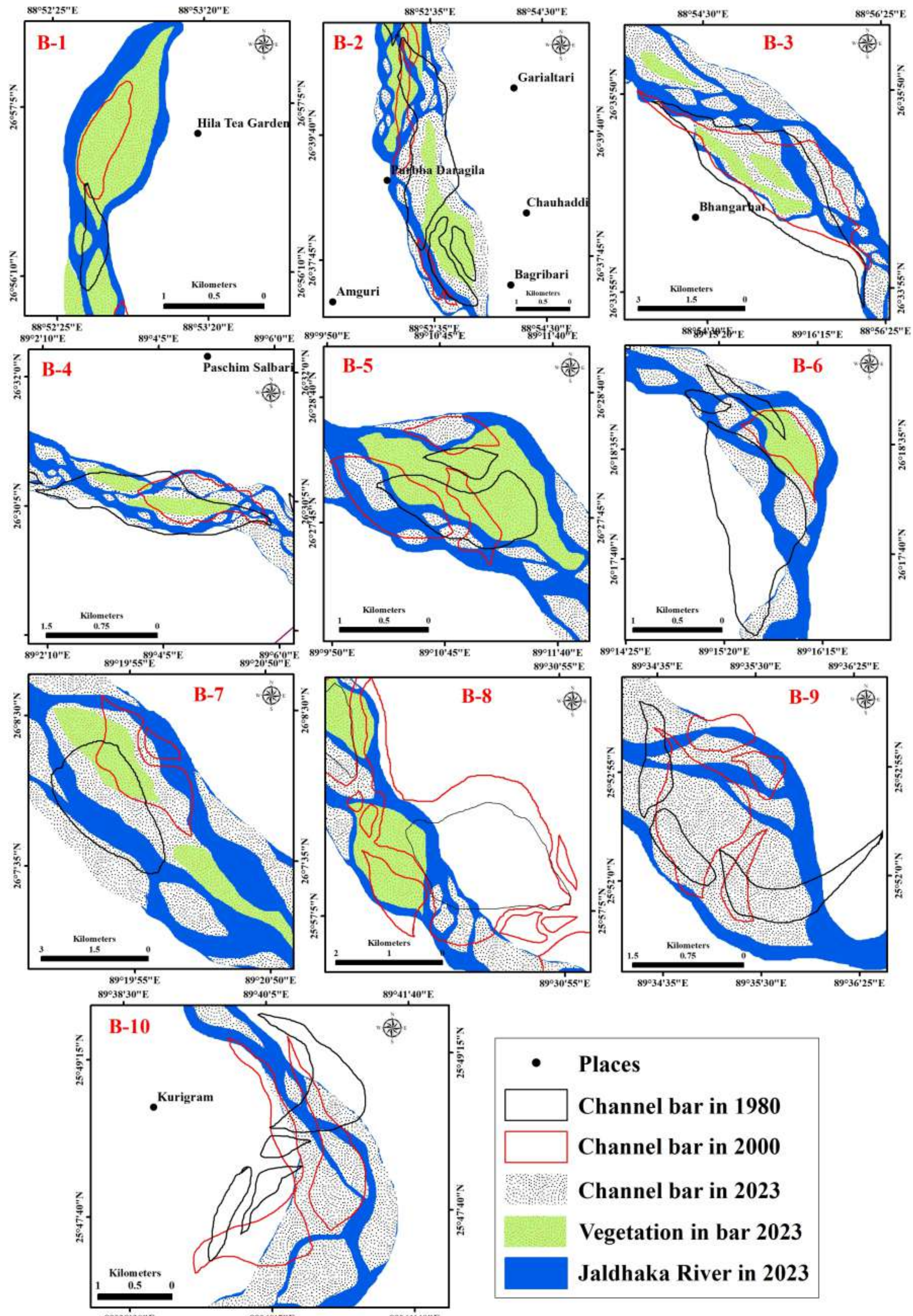

B-1
Hila Tea Garden
B-2
Garialtari
Purbba Daragila
Chauhaddi
Bagribari
Amguri
B-3
Bhangarhat
B-4
Paschim Salbari
B-5
B-6
B-7
B-8
B-9
B-10
Kurigram
Kilometers
Places
Channel bar in 1980
Channel bar in 2000
Channel bar in 2023
Vegetation in bar 2023
Jaldhaka River in 2023

◂**Fig. 9** Changes of morphological attributes of ten selected channel bars located (B1-near Hila tea garden; B2-near Amguri; B3-near Bhangarhat; B4-near Jore Simuli; B5-near Mukuldanga; B6-at Brahmattar Sanatali near Nishiganj; B7-near Adabari Ghat of Singimari River; B8-near Kulaghat; B9-near Holokhana; B10-near Kurigram) in the Jaldhaka River. It has been observed that this bar is turned into a mid-channel bar from a point bar and shape has also been changed from oval to elliptical within the studied period. Results showed that the length of the B7 bar has been gradually reduced during the studied period and width (the width of this bar was 0.86 km. in 1980) also decreased in 2000 (0.43 km). Moreover, the width has been increased in 2023 (0.92 km). In the case of B8 bar (located near Kulaghat), the results indicated that the length was 3.36 km in 1980 and the width was 2.06 km and the area was 4.31 km^2 but in 2000, the bar area (7.81 km^2), length (5.73 km), width (3.25 km) perimeter (15.75 km) were drastically increased with irregular shapes (Table 4; Figs. 10 and 11). An increasing trend in bar area has been noticed for B9 which has turned from a crescent-shaped mid-channel bar (1980) to an elongated sidebar (2023) within the studied timeframe. Lastly, the bar B10 was 3.3 km long in 1980 but gradually it extended its length in 2000 (4.98 km) and 2023 (5.98 km) towards downstream while the area of this bar also increased over time

Variation and distribution of sediment grain size

Grain size has been estimated and analyzed for the eleven samples of the Jaldhaka River. Those samples were collected from the river bed of each sub-reach. The grain size of the channel bed varies with channel gradient, flow velocity, discharge and sediment supply. The results indicated significant changes in grain size (%) in the Jaldhaka river bed materials (Fig. 12b). The sample S-1 (from sub-reach 1 that falls under the lesser Himalayan region) reveals 30.20% cobble, 25.30 very coarse to fine pebble and gravel, 32.30 granule materials and 12.20 of coarse to fine sand with the absence of silt and clay. Samples S-2 and S-3 (collected from the Piedmont region) contain the cobble, very coarse to fine pebbles, granules, and coarse sand. Samples S-4, S-5, and S-6 contain small amounts of clay, silt, and a large amount of fine to coarse-grained sand, granule, and gravel materials. On the other hand, the finer-grained material concentration is higher in the case of the samples S-7, S-8, S-9, S-10, and S-11 collected from the downstream sub-reaches of the River Jaldhaka (Table 8). Here, grain size volume in percentage value is plotted against each of the samples (Fig. 12a).

Descriptive statistics have been calculated to understand the nature of grain size datasets (Table 9). Results showed that samples of the lower sub-reaches contain moderately sorted bed material but out of 11 samples, sample 3 is poorly sorted (Fig. 12b).

Discussions

Channel morpho-dynamics are controlled by natural geomorphic processes, climatic conditions, flow regime, sediment transportation, deposition, and human interference (mainly pattern of land use (Saha et al. 2022). Different morpho-dynamic variables are responsible for the spatiotemporal alterations of channel bars in the Jaldhaka River which flows through the Eastern Himalayan Foreland Basin (EHFB) area. This present study considers the sub-reaches of transboundary River Jaldhaka under the flowing part of India (Kalimpong, Jalpaiguri, and Coochbehar district of West Bengal) and Bangladesh (Lalmonirhat and Kurigram district) up to its confluence with Jamuna (Brahmaputra) River. The channel bars of the Jaldhaka River have been continuously modified through the in-stream erosion-accretion dynamics.

Channel braiding nature in the Jaldhaka River

The Jaldhaka River planform is mainly braided in nature and the average sinuosity value is low (Sarkar and Bera 2024) (varies between 1.01 and 1.32 in 1980, 1.02 to 1.40 in 2000 and 1.02 to 1.36 in 2023 among all considering sub-reaches) which indicated less sinuous (closer to straight) channel flow path. The Jaldhaka River has a straight to sinuous channel in the upper sub-reach in Sikkim and Bhutan, but it has formed moderate to higher braided planform after entering West Bengal. Interestingly, the lower sub-reaches such as SR-10 (located near Chhinaihat) and SR-11 (near Kurigram) have comparatively higher SI values than the upper sub-reaches (SR-3and SR-4). The higher SI value indicated that the channel has been experiencing a low channel gradient with lower channel energy and minimal sediment deposition. Channel dynamics have been observed after 1980 in the lower sub-reaches (in between Mathabhanga and Bagua Anantapur) due to significant variation of channel discharge in monsoon and post-monsoonal months, engagements of a large number of tributaries from both sides of Jaldhaka, thalweg line shifting, relaxation of channel energy with the formation of meander scars and cut-offs and huge anthropogenic modifications (rapid growing settlements and changes in land use in the Kurigram district (Sarkar et al. 2021) etc. The Quaternary non-cohesive bank materials, active channel oscillation by shifting (leads to erosion-accretion) (Sarkar and Bera 2022) of thalweg and aggradation of sediments are responsible for braided morphology of the Jaldhaka River. The shape of the channel bar varies with changing bar length, width, perimeter, and area within the study period. The average channel area in 1980 was moderate compared with 2000 because of a massive frequent flood event that occurred in this area in 1996 (maximum water level was 0.42 m above

Table 3 Reach-wise channel morphological parameters of Jaldhaka River in 1980, 2000, and 2023

Year	Sub-reach id	Reach length in km	Straight length in km (*SL*)	Total bar count (*TBC*)	Total bar area in km^2 (*TBA*)	Total vegetated area in km^2 (*TVA*)	Total channel area (*TCA*) including bars in km^2	Total channel area excluding bars in km^2 (*TCA*)	Flow top width (*T*) in km^2	Bank to bank (B_b) in km^2	Total braided channel (*N*)
1980	SR-1	46.00	40.23	–	–	–	–	–	–	–	–
	SR-2	21.82	20.43	16	5.56	6.76	24.89	12.57	0.46	1.41	3
	SR-3	18.65	18.45	14	15.87	5.97	36.18	14.34	0.42	1.30	4
	SR-4	11.93	11.81	9	9.45	0.74	12.54	2.35	0.72	1.22	3
	SR-5	16.45	15.47	12	15.94	0.76	22.99	6.29	0.68	1.10	2
	SR-6	20.14	15.42	13	9.17	9.36	27.20	8.67	0.69	1.21	2
	SR-7	25.05	24.19	22	15.24	2.23	30.38	12.91	0.60	0.95	3
	SR-8	16.12	15.26	19	10.73	3.06	22.24	8.45	0.45	1.15	2
	SR-9	18.90	18.02	13	3.13	13.85	29.95	12.97	0.63	1.02	3
	SR-10	21.26	16.15	18	7.04	0.00	19.99	12.95	0.42	1.22	2
	SR-11	20.94	17.87	15	7.21	0.00	18.05	10.84	0.51	1.05	2
2000	SR-1	46.02	40.05	–	–	–	–	–	–	–	–
	SR-2	21.78	20.24	13	5.84	3.46	23.38	14.08	0.68	1.32	4
	SR-3	18.30	18.00	11	8.65	5.02	33.69	20.02	0.52	1.44	3
	SR-4	12.45	12.09	9	9.61	0.00	15.03	5.42	0.45	0.85	2
	SR-5	16.25	15.75	13	12.23	7.54	27.65	7.88	0.49	0.95	3
	SR-6	20.32	16.02	15	14.29	7.06	29.40	8.05	0.56	1.11	3
	SR-7	25.00	24.55	17	19.03	5.36	37.78	13.39	0.52	0.92	3
	SR-8	15.67	15.05	22	12.97	3.25	24.75	8.53	0.51	0.82	2
	SR-9	18.85	17.00	13	13.09	5.69	35.73	16.95	0.62	1.02	3
	SR-10	20.24	16.25	16	16.56	0.00	26.87	10.31	0.46	0.95	3
	SR-11	22.60	16.18	12	13.88	0.00	23.48	9.60	0.57	0.81	3
2023	SR-1	45.98	40.06	–	–	–	–	–	–	–	–
	SR-2	21.67	20.21	30	2.36	5.89	16.55	8.30	0.45	1.10	4
	SR-3	18.97	18.20	24	5.34	7.24	23.90	11.32	0.41	0.89	4
	SR-4	12.08	11.69	12	7.41	0.94	12.86	4.51	0.31	0.75	3
	SR-5	15.96	15.64	32	13.93	3.99	22.34	4.42	0.29	0.85	3
	SR-6	20.40	15.34	28	10.41	2.53	24.07	11.13	0.68	1.07	2
	SR-7	25.05	24.26	30	17.36	6.39	36.13	12.38	0.58	0.96	3
	SR-8	16.02	15.23	18	14.98	1.88	23.91	7.05	0.42	0.82	3
	SR-9	18.75	17.90	21	9.45	6.34	25.65	9.86	0.48	0.84	2
	SR-10	20.51	16.47	18	14.79	2.76	25.87	8.32	0.55	0.90	3
	SR-11	22.48	16.52	16	12.73	0.00	21.12	8.39	0.43	0.75	2

Table 4 Spatiotemporal alteration of morphological attributes of ten selected bars in Jaldhaka River

Year	Parameter	B1	B2	B3	B4	B5	B6	B7	B8	B9	B10
1980	Bar length (km)	1.05	8.28	5.88	6.47	2.05	3.35	1.66	3.36	3.34	3.3
	Bar width (km)	0.48	1.13	1.37	1.64	1.01	1.3	0.86	2.06	0.47	1.1
	Bar shape	Oval	Elongated	Elongated	Elongated	Irregular	Triangular	Oval	Oval	Crescentic	Crescentic
	Bar Perimeter (km^2)	2.48	13.31	11.39	13.47	5.26	7.76	4.35	8.17	6.68	7.85
	Bar Area (km^2)	0.35	3.82	3.37	5.79	1.6	2.85	1.12	4.31	1.09	2.8
	Bar type	Mid channel	Point bar	Point bar	Point bar	Transverse	Point bar	Mid channel	Point bar	Mid channel	Point bar
2000	Bar length (km)	1.21	6.68	5.17	3.66	2.36	1.62	1.82	5.73	2.78	4.98
	Bar width (km)	0.35	0.29	1.41	1.45	0.79	0.6	0.43	3.25	1.44	0.35
	Bar shape	Oval	Elongated	Elongated	Rhomboid	irregular	Oval	Irregular	Irregular	irregular	Irregular
	Bar Perimeter (km^2)	2.72	8.03	11.37	8.33	4.65	4.07	4.39	15.75	7.02	11.71
	Bar Area (km^2)	0.32	4.39	3.16	3.03	1.36	0.96	0.79	7.81	2.07	3.06
	Bar type	Mid channel	Point bar	Point bar	Mid channel	Transverse	Mid channel	Point bar	Point bar	Lateral bar	Side bar
2023	Bar length (km)	1.53	5.98	2.65	3.47	3.45	2.19	3.28	2.01	5.48	5.98
	Bar width (km)	0.67	1.51	1.11	0.93	1.36	0.77	0.92	0.62	1.53	1.11
	Bar shape	Elliptical	Elongated	Irregular	Squared	irregular	Elliptical	Elongated	Irregular	Elongated	Irregular
	Bar Perimeter (km^2)	4.71	13.42	6.36	7.69	8.21	5.57	8.54	4.1	11.64	11.35
	Bar Area (km^2)	0.86	7.08	1.75	2.54	2.53	1.88	2.05	3.11	5.26	3.11
	Bar type	Mid channel	Point bar	Transverse	Mid channel	Mid channel	Mid channel	Mid channel	Point bar	Side bar	Point bar

Fig. 10 Diversity in shape of channel bar along the different sub-reaches of braided River Jaldhaka

danger level), 1998 (0.35 m above danger level) and 2000 (0.10 m above danger level) as per the annual flood report of 1996 to 2000.The SR-2 and SR-3 experienced a sudden drop in channel gradient (10.32 m/km in between Nagrakata Tea Garden and Tandu village) with multiple irregularly shaped mid-channel bars and point bars which are located exactly south of the southernmost extent of the Himalayan Mountain front (Himalayan Frontal Thrust). The middle reach of the Jaldhaka has also experienced frequent flood occurrences which have led to the modification of the floodplain as well as channel bars. However, recent research on channel braiding forecast through ARIMA modeling revealed that the middle reach of the Jaldhaka River is more prone to braiding compared to other reaches (Saha et al. 2022).

The wider channel path with a higher number of channel nodes and bifurcation has been noticed in the middle sub reaches of the Jaldhaka River in the case of SR-4, 5, and 6 (areas located from Ramsai to Mukuldanga section of the Jaldhaka River) which are shown higher BI value from 1980 to 2023. Contrarily, the geomorphological setting of

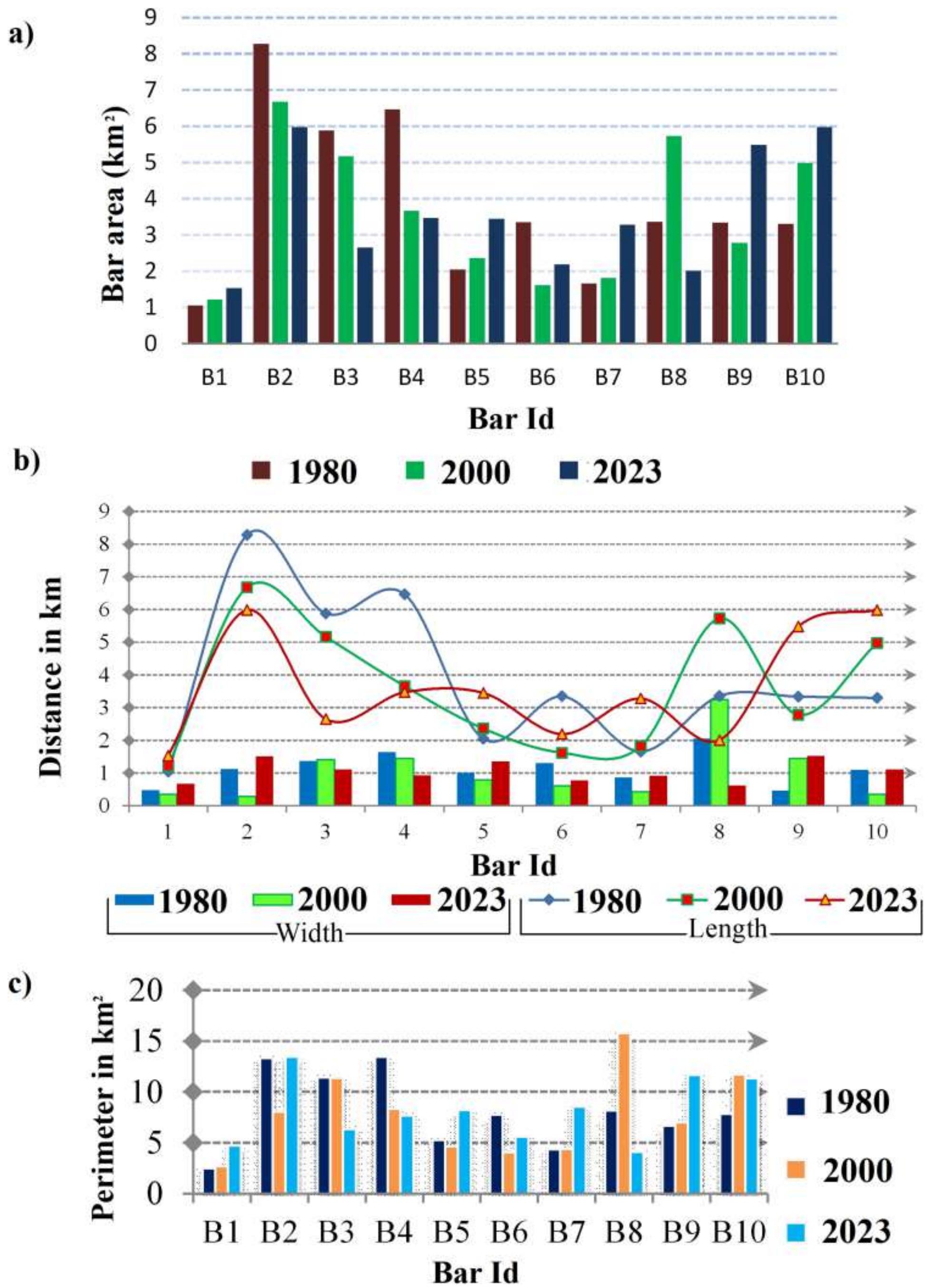

Fig. 11 Dynamicity in channel bar morphological parameters; **a** Variation in channel bar area in 1980, 2000, and 2023, **b** Changing channel bar width and length, **c** Spatio-temporal changes of channel bar perimeter in 1980, 2000, and 2023

the middle sub-reaches of the Jaldhaka basin are comprised of the mid-altitude proximal fan, Quaternary floodplain and younger alluvium which is dominating causes of frequent alteration of channel bars. SR-2 and 3 (located at the Piedmont section i.e. Nagrakata, Sulkapara, Khairbari, Tandu, Bamandanga region of Jalpaiguri) indicated the higher braiding intensity in terms of low PFI value over the study period (Sarkar and Bera 2024). Excessive river bank erosion, formation of spill channels, local meandering channels, and non-cohesive bank materials of the Jaldhaka river basin are responsible for the bar alteration in the middle and lower reaches. On the other hand, huge sediment loads deposition in-stream shallow pool-riffle sequence, presence of vegetation or any obstacles to dropping the sediment led to the development of a channel bar in the Jaldhaka River.

Table 5 Variations of channel and braiding indices over the study time frame (1980 to 2023)

Year	Sub-reach	*BI*	*TBI*	*SI*	*SIT*	*PFI*	*FGI*	*ND*
1980	SR-1	–	–	1.14	–	–	–	–
	SR-2	3.55	1.42	1.07	2.12	10.87	6.49	2.85
	SR-3	2.49	1.54	1.01	2.31	12.50	8.96	2.00
	SR-4	2.40	1.64	1.01	1.94	19.70	5.98	3.93
	SR-5	2.52	0.91	1.06	2.10	30.91	4.42	5.39
	SR-6	2.10	1.65	1.31	2.03	28.51	3.78	5.40
	SR-7	2.22	1.05	1.04	1.39	21.05	5.86	3.25
	SR-8	2.85	1.74	1.06	1.80	19.57	3.69	2.97
	SR-9	3.02	0.98	1.05	1.42	20.59	5.85	2.41
	SR-10	2.18	0.82	1.32	1.97	17.21	3.23	2.07
	SR-11	2.09	0.95	1.17	1.19	24.29	3.52	1.42
2000	SR-1	–		1.15	–	–	–	–
	SR-2	3.15	2.27	1.08	2.07	12.88	11.56	3.71
	SR-3	2.42	1.39	1.02	2.21	12.04	5.91	3.21
	SR-4	2.45	2.34	1.03	1.93	26.49	5.94	3.36
	SR-5	2.15	2.11	1.03	1.92	17.09	9.22	3.24
	SR-6	2.22	0.90	1.27	1.74	16.67	6.98	4.90
	SR-7	2.30	1.09	1.02	1.33	18.84	7.55	2.28
	SR-8	2.74	1.22	1.04	1.83	31.10	5.17	1.58
	SR-9	3.00	1.96	1.11	1.71	20.26	6.73	1.23
	SR-10	2.15	1.05	1.25	1.79	16.07	6.71	1.66
	SR-11	2.06	1.23	1.40	1.13	23.46	8.34	1.03
2023	SR-1	–		1.15	–	–	–	–
	SR-2	3.53	1.82	1.07	2.00	10.23	14.86	5.25
	SR-3	2.72	1.12	1.04	2.09	11.52	13.27	1.89
	SR-4	2.30	2.67	1.03	1.93	13.78	9.80	2.87
	SR-5	2.55	3.13	1.02	2.01	11.37	9.88	4.73
	SR-6	2.20	0.93	1.33	1.70	31.78	4.74	3.50
	SR-7	2.14	1.04	1.03	1.29	20.14	6.96	2.61
	SR-8	2.91	1.22	1.05	1.73	17.07	8.45	2.10
	SR-9	3.16	1.19	1.05	1.73	28.57	6.81	1.36
	SR-10	2.46	1.11	1.25	1.77	20.37	7.79	2.04
	SR-11	2.10	1.33	1.36	1.12	28.67	6.37	1.07

Table 6 Cross-section wise fluvio-hydrological attributes of the Jaldhaka River in post-monsoonal months (November–December) of 2022

Cross section	Water level (m)	Average velocity (m/s)	Total width (m)	Flow top width (m)	Wetted perimeter (m)	Cross-sectional area (Sq.m)	Average depth in m(A/P)	Total discharge (m^3/s)	Slope (S)	Manning coefficient	C-Chezy	W-D ratio
a–a′	25.63	0.71	1596	449.33	409.33	408.67	1.00	288.52	0.00016	0.025	41.52	1598.57
b–b′	25.63	0.72	1820	459.50	460.50	450.91	0.98	323.76	0.00016	0.025	41.87	1858.70
c–c′	25.63	0.63	1560	550.65	550.45	550.79	1.00	344.25	0.00016	0.024	41.59	1559.02
d–d′	26.05	0.52	1400	509.36	509.26	518.99	1.02	267.28	0.00015	0.024	41.53	1373.76
e–e′	26.04	0.50	1500	608.00	608.00	609.14	1.00	305.79	0.00015	0.025	40.81	1497.20
f–f′	26.04	0.59	1200	622.36	622.36	614.10	0.99	363.55	0.00015	0.025	40.08	1216.14
g–g′	26.25	0.49	1556	609.00	609.00	653.95	1.07	321.09	0.00014	0.025	40.09	1449.05
h–h′	26.35	0.48	1560	633.25	633.25	648.95	1.02	312.80	0.00014	0.025	40.16	1522.25
i–i′	26.60	0.48	1460	608.50	608.70	642.12	1.05	308.22	0.00014	0.025	40.50	1384.02

Table 7 Cross-section wise fluvio-hydrological attributes of the Jaldhaka River in monsoonal months (July–August) of 2023

Cross section	Water level (m)	Average velocity (m/s)	Total width (m)	Flow top width (m)	Wetted perimeter (m)	Cross-sectional area (Sq.m)	Average depth in m(A/P)	Total discharge (m^3/s)	Slope (S)	Manning coefficient	C-Chezy	W-D ratio
a–a′	30.23	1.32	1600	635.32	635.85	1324.53	2.08	1748.37	0.00035	0.032	34.65	768.09
b–b′	30.25	1.37	1822	625.36	625.35	1345.38	2.15	1843.17	0.00035	0.029	39.14	846.89
c–c′	30.60	1.38	1562	678.65	678.67	1524.35	2.25	2103.60	0.00035	0.034	37.58	695.43
d–d′	28.69	1.10	1408	767.39	768.36	1748.53	2.28	1923.38	0.00035	0.035	33.12	618.72
e–e′	28.90	1.12	1500	925.36	925.36	1898.67	2.05	2126.51	0.00035	0.034	33.86	731.06
f–f′	28.90	1.20	1220	785.63	785.60	1825.33	2.32	2190.40	0.00035	0.034	33.25	525.07
g–g′	28.40	1.02	1560	854.32	854.52	1836.26	2.15	1878.86	0.00035	0.032	34.65	725.96
h–h′	28.45	0.96	1566	925.36	926.43	2107.42	2.27	2012.59	0.00035	0.029	39.14	688.42
i–i′	28.35	0.95	1480	878.65	788.55	1541.03	1.95	1459.36	0.00035	0.034	37.58	757.32

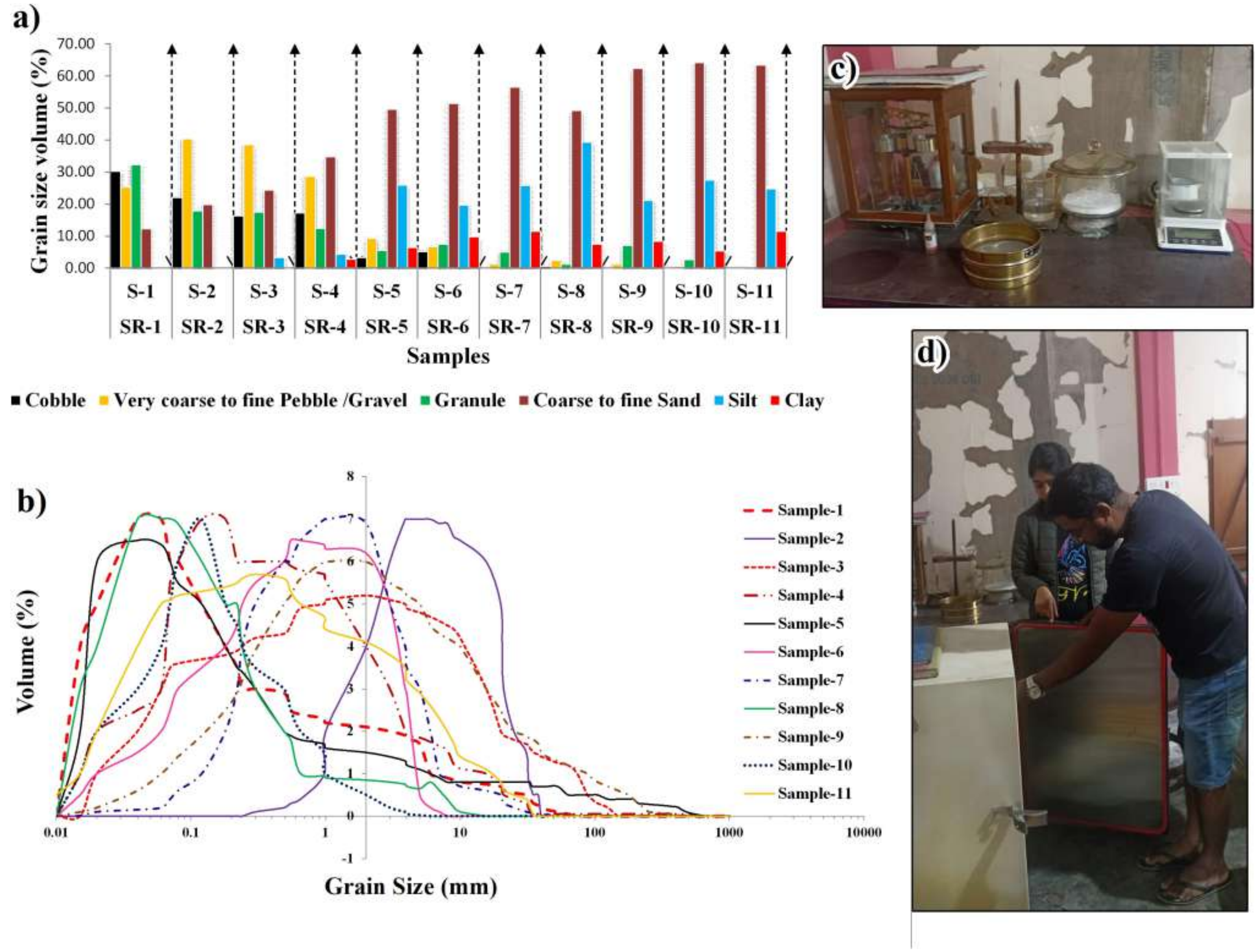

Fig. 12 Grain size analysis of eleven samples of channel bar in the Jaldhaka River **a** Samples grain size volume in percentage (%), **b** Grain size distribution curve, **c** and **d** Photographs were taken during grain size analysis in the laboratory

Table 8 Volume (%) of grain size of bed materials in Jaldhaka River under collected samples (eleven samples)

Channel sub-reach	Sample	Cobble	Very coarse to fine pebble/gravel	Granule	Coarse to fine sand	Silt	Clay
SR-1	S-1	30.20	25.30	32.30	12.20	0.00	0.00
SR-2	S-2	22.05	40.36	17.79	19.80	0.00	0.00
SR-3	S-3	16.30	38.60	17.46	24.36	3.28	0.00
SR-4	S-4	17.21	28.60	12.42	34.74	4.31	2.72
SR-5	S-5	3.25	9.30	5.50	49.60	25.90	6.45
SR-6	S-6	5.16	6.72	7.40	51.43	19.58	9.71
SR-7	S-7	0.00	1.20	5.04	56.46	25.80	11.50
SR-8	S-8	0.50	2.40	1.20	49.20	39.32	7.38
SR-9	S-9	0.00	1.20	7.01	62.36	21.10	8.33
SR-10	S-10	0.00	0.50	2.61	64.15	27.42	5.32
SR-11	S-11	0.00	0.20	0.31	63.36	24.68	11.45

Table 9 Descriptive statistics of sediment grain size distribution of river bed (eleven samples) of the Jaldhaka

Descriptive statistics	S-1	S-2	S-3	S-4	S-5	S-6	S-7	S-8	S-9	S-10	S-11
Mean	0.867	0.945	1.329	1.079	0.952	0.834	0.802	0.711	1.316	0.564	1.086
Standard error	0.165	0.213	0.184	0.202	0.156	0.187	0.182	0.174	0.185	0.145	0.189
Standard deviation	1.641	2.119	1.828	2.006	1.518	1.862	1.813	1.734	1.836	1.446	1.879
Sample variance	2.691	4.490	3.342	4.026	2.305	3.468	3.285	3.008	3.372	2.090	3.532
Kurtosis	4.638	3.191	-0.558	2.164	5.520	3.193	4.758	6.436	0.486	6.987	0.663
Skewness	2.263	2.180	1.027	1.896	2.461	2.142	2.433	2.721	1.327	2.750	1.508
Range	7.000	7.000	5.200	7.000	6.500	6.500	7.000	7.010	6.000	7.000	5.700
Minimum	0.000	0.000	0.000	0.000	0.000	0.000	0.000	0.000	0.000	0.000	0.000
Maximum	7.000	7.000	5.200	7.000	6.500	6.500	7.000	7.010	6.000	7.000	5.700

Relationships between fluvio-hydrological parameters and channel braiding

Variability of water depth, channel velocity, channel slope, wetted perimeter, flow top width, channel width, channel discharge etc. have been responsible factors that make complex braiding environment in the Himalayan-origin alluvial transboundary River Jaldhaka within the foreland basin area (Ghosh et al. 2022). However, the distinct pattern of fluvio-hydrological parameters in post-monsoon and monsoon (Fig. 13) has remarkably different which can cause seasonal alteration of the channel bar in the Jaldhaka River. Frequency, magnitude, seasonality, duration, sediment supply etc. have been strongly related to the spatiotemporal dynamics of morphological attributes (bar length, width, perimeter area) of the channel bar in Jaldhaka River.

Controlling factors of spatiotemporal channel bar morpho-dynamics and its consequences

Long-term changes of channel bar in different reaches of the Jaldhaka have been assessed but the main causes of alteration vary in different reaches. The tectonically active the Himalayan region is characterized by several active faults and thrust. The upper reaches of the Jaldhaka are dominated by many uplifted tectonic unpaired river terraces and the channel is more confined than the lower reaches. However, the river systems influenced by active tectonics (Gansser 1964; Goswami et al. 2012) make different types of channel configurations in this region. Additionally, the river Jaldhaka is tremendously altered from a narrow deep-valley like planform to a complete braided avulsive channel towards the downstream direction beyond the Himalayan Frontal Thrust (southernmost extent of Nagrakata and Thaljhora scarp). Previous research has also revealed the tectonic and climatic control on the fluvial system of the Piedmont section of Eastern Himalaya. Active tectonic imprints like thrust, fault, and lineaments trigger the dynamicity (lateral migration of channel) in the channel belt that influences in sedimentation processes of the channel.

Lastly, human interference like changing land use patterns, intensive agriculture practices (in point bar near Bhangarhat, Kasheti, Sarhati), the establishment of human settlements (in the bar near Dobbari village, Rangamati near Mukuldanga, bar near Gitaldaha, Dakshin Singimari and Holokhana), channel bed sand mining (near Ghoksadanga) and different longitudinal, cross-sectional engineering works along and across the river are the principal causes of spatiotemporal alteration of channel bar. Various researchers highlighted that sand and gravel mining are also causes of channel bed alteration and thalweg shifting in the Himalayan foreland plain area. However, previous research focused on the fast-changing landscape of the Himalayan Foreland Basin area is experienced by large-scale deforestation and sediment yield (Chamling et al. 2021; Ghosh et al. 2022).

Role of sediments grain size in bar dynamics

High altitudinal mountainous region is the storehouse of sediments which tends to drop as river carried load with the alteration of channel gradient. Excessive rainfall accelerates sediment yield and settling velocity intricates the accumulation of sediments in the channel bed. Different shape of channel bars varies in case of different ranges of channel velocity and discharge. Additionally, varying sediment grain size plays a significant role in sediment sorting, flow resistance, bar stability, and morphology (shapes) (Fig. 10). However, the channel bifurcation occurs in the foothill section and dropped debris (with a larger diameter) which makes the channel bar (generally boulder or gravel bars). So, multiple-shaped rivers carried materials are responsible for the bar dynamics of the Jaldhaka River. Large boulder, gravel, pebble to coarser-grained channel bed materials dominate in the sub-reaches near the Piedmont section. Similarly coarser to finer-grained sand to silt materials is dominant in the channel bar of middle

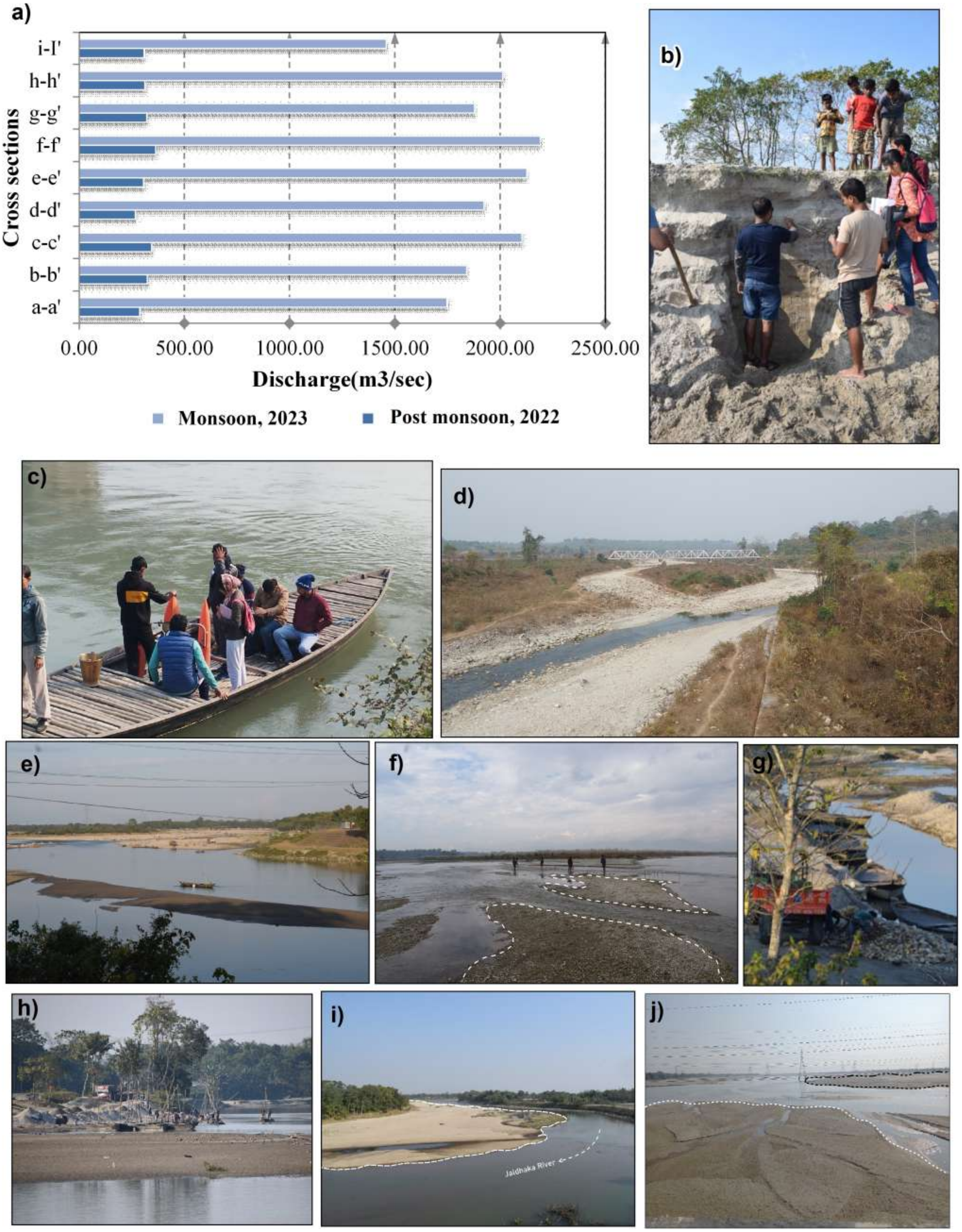
a)
Cross sections
i-I'
h-h'
g-g'
f-f'
e-e'
d-d'
c-c'
b-b'
a-a'
0.00
500.00
1000.00
1500.00
2000.00
2500.00
Discharge(m3/sec)
Monsoon, 2023
Post monsoon, 2022
b)
c)
d)
e)
f)
g)
h)
i)
Jaldhaka River
j)

◂**Fig. 13** **a** Variation in river discharge of the Jaldhaka during post-monsoon and Monsoon season, **b** Photographs were taken during sediment sample collection phase, **c** Use of ADCP during field investigation, **d** Gravel bar (mid-channel) formation near Nagrakata, **e** Longitudinal bar formation, **f** Formation of lateral and transverse bar, **g and h** Sand mining site in Jaldhaka River near Ghoksadanga, **i** Development of point bar at a concave bank of Jaldhaka River near Betgara, **j** Bar formation at the confluence of Diana and Jaldhaka River

sub-reaches but lower most sub-reaches are dominated by the silt and clay materials. The floodplain of middle sub-reaches near Dhupguri to Mathabhanga segments is composed of non-cohesive (unconsolidated) materials so the river sub-reaches are prone to frequent channel shifting and bar modification. Rapid shifting of active channels through erosion and accretion influences the shape, size and types of channel bar.

Conclusion

The present study has been assessed through a detailed spatiotemporal dynamics of channel bars with the help of geospatial datasets of the last 43 years (1980–2023) and field datasets of recent years (2022–2023) in the Jaldhaka river system. Several channel indices have been calculated to quantify the channel dynamics and braiding intensity in the braided sub-reaches of the Jaldhaka River. Results show the lower sub-reaches (Mathabhanga to Bagua Anantapur segment) of the Jaldhaka are more dynamic than other upper sub-reaches but braid bars of Jaldhaka in the middle sub-reaches are most dynamic within the channel belt over the study timeframe. Based on the results section it can be concluded that the dynamic Himalayan Rivers carry ample amount of water, sediments and drop below the Piedmont section which makes higher braiding intensity. The channel bifurcation mostly occurred in this region and multiple flow paths make different shaped channel bars. Here, SR-3 and SR-4 indicated higher BI, low PFI and low SI values which means the channel braiding possibly happens due to changing gradient (Ghosh et al. 2023e; Sarkar and Bera 2024). The loss of vegetation cover makes the channel bar more dynamic in the lower reaches of the Jaldhaka with time. This present study identifies the variability in river discharge during monsoon and post-monsoon. The braiding of the Jaldhaka River incorporated the frequent alteration of the channel bar within the channel belt which indicates the channel belt is partially confined. Changes in sub-reaches highlight the control of local factors that alter the channel bar within the study period of 1980 to 2023. Planimetric and geometric assessments of channel and bar dynamics are very crucial to know for any kind of construction work in the river corridor. So, this paper gives some insights into the causes and consequences of channel bar dynamics to get some knowledge about it. However, proper channel belt management can minimize the negative consequences of frequent channel bar dynamism in the Jaldhaka River.

Author contributions B. Bera conceptualized, supervised, edited and modified the whole manuscript. S. Sarkar acquired, analyzed, visualized data and wrote the draft manuscript.

Funding There is no funding for this investigation.

Data availability The data that support the findings of this study are available on request from the corresponding author upon reasonable request.

Declarations

Competing interests The authors declare that they have no known competing financial interests or personal relationships that could have appeared to influence the work reported in this paper.

Ethical approval Both authors have read and understood the "Ethical Responsibilities of Authors" and have complied with these guidelines where applicable, as outlined in the Instructions for Authors.

Consent to participate Not applicable.

Consent to publish All authors consent to the publication of this research.

References

Akhter, S., Eibek, K.U., Islam, S., Islam, A.R.M.T., Chu, R., Shuanghe, S.: Predicting spatiotemporal changes of channel morphology in the reach of Teesta River, Bangladesh using GIS and ARIMA modeling. Quat. Int. **513**, 80–94 (2019). https://doi.org/10.1016/j.quaint.2019.01.022

Ashmore, P.: Channel morphology and bed load pulses in braided, gravel-bed streams. Geografiska Annaler Ser.: A Phys. Geogr. **73**(1), 37–52 (1991). https://doi.org/10.1080/04353676.1991.11880331

Ashmore, P.: Morphology and dynamics of braided rivers (2013). https://doi.org/10.1016/B978-0-12-374739-6.00242-6.

Ashworth, P.J.: Mid-channel bar growth and its relationship to local flow strength and direction. Earth Surf. Process. Landf. **21**(2), 103–123 (1996)

Bera, B., Bhattacharjee, S., Roy, C.: Estimating stream piracy in the lower Ganga Plain of a Quaternary geological site in West Bengal, India applying sedimentological bank facies, log and geospatial techniques. Curr. Sci. **117**(4), 662–671 (2019)

Bera, B., Bhattacharjee, S., Sengupta, N., Chamling, M., Ghosh, S., Ghosh, A.: Impacts of channelization of River Bala, eastern Himalayan foothills, India. Geol. Ecol. Landsc. (2022). https://doi.org/10.1080/24749508.2022.2130857

Bertoldi, W., Zanoni, L., Tubino, M.: Planform dynamics of braided streams. Earth Surf. Process. Landf. **34**(4), 547–557 (2009). https://doi.org/10.1002/esp.1755

Brice, J.C.: Channel patterns and terraces of the Loup Rivers in Nebraska. United States Government Printing Office. Geol. Surv. Prof. Pap. **422-D**, D1–D41 (1964). https://doi.org/10.3133/pp422D

Chakraborty, S., Datta, K.: Causes and consequences of channel changes—a spatio temporal analysis using remote sensing and GIS—Jaldhaka-Diana River System (Lower Course), Jalpaiguri (Duars), West Bengal, India. J. Geogr. Nat. Disast. **3**(1), 1–13 (2013). https://doi.org/10.4172/2167-0587.1000107

Chamling, M., Bera, B., Sarkar, S.: Geospatial environmental modeling of forest declining trend in Eastern Himalayan biodiversity hotspot region. In: Forest Resources Resilience and Conflicts, pp. 417–433. Elsevier (2021). https://doi.org/10.1016/B978-0-12-822931-6.00030-7

Chamling, M., Bera, B., Sarkar, S.: Large-scale human intervention and estimation of flood susceptibility applying frequency ratio model. In: Spatial Modelling of Flood Risk and Flood Hazards: Societal Implications, pp. 161–183. Springer International Publishing, Cham (2022). https://doi.org/10.1007/978-3-030-94544-2_10

Charlton, R.: Fundamentals of Fluvial Geomorphology. Routledge, London (2007)

Church Mand Jones, D.: Channel bars in gravel bed rivers. In: Hey, R.D., Bathurst, J.C., Thorne, C.R. (eds.) Gravel Bed Rivers, pp. 291–338. Wiley, Chichester (1982)

Dey, S., Ali, S.Z.: Fluvial instabilities. Phys. Fluids (2020). https://doi.org/10.1063/5.0010038

Duro, G., Crosato, A., Tassi, P.: Numerical study on river bar response to spatial variations of channel width. Adv. Water Resour. **93**(25), 21–38 (2015). https://doi.org/10.1016/j.advwatres.2015.10.003

Egozi, R., Ashmore, P.: Defining and measuring braiding intensity. Earth Surf. Process. Landf. **33**(14), 2121–2138 (2008). https://doi.org/10.1002/esp.1658

Friend, P.F., Sinha, R.: Braiding and meandering parameters. Geol. Soc. Spec. Publ. **75**(1), 105–111 (1993). https://doi.org/10.1144/GSL.SP.1993.075.01.05

Gansser, A.: Geology of the himalayas (1964)

Germanoski, D., Schumm, S.A.: Changes in braided river morphology resulting from aggradation and degradation. J. Geol. **101**(4), 451–466 (1993). https://doi.org/10.1086/648239

Ghosh, S., Bera, B.: River Raidak-I migration dynamics within Himalayan foreland basin applying Quaternary sedimentological bank facies and Geospatial techniques. In: Drainage Basin Dynamics: An Introduction to Morphology, Landscape and Modelling, pp. 153–177 (2022). https://doi.org/10.1007/978-3-030-79634-1_7

Ghosh, S., Saha, S., Bera, B.: Flood susceptibility zonation using advanced ensemble machine learning models within Himalayan foreland basin. Nat. Hazard. Res. **2**(4), 363–374 (2022). https://doi.org/10.1016/j.nhres.2022.06.003

Ghosh, S., Mandal, P., Bera, B.: Geospatial and fluvio-geomorphological investigation of confluence dynamics of river Raidak within Himalayan foreland basin, India. Phys. Geogr. **44**(2), 207–241 (2023a). https://doi.org/10.1080/02723646.2022.2068405

Ghosh, S., Mandal, P., Bera, B.: Chronological evolution of Holocene floodplain of river Raidak within the Himalayan foreland basin, India. Quat. Sci. Adv. **10**, 100076 (2023b). https://doi.org/10.1016/j.qsa.2023.100076

Ghosh, S., Mandal, P., Bera, B.: Dynamics of channel bar morphology on multi-decadal timescales in a braided river within Himalayan foreland basin, India. J. Earth Syst. Sci. **132**(4), 168 (2023c). https://doi.org/10.1007/s12040-023-02187-x

Ghosh, S., Mandal, P., Bera, B.: Dynamics of meander geometry and formation of neck cutoff of river Raidak-I within Himalayan foreland basin, India. J Geol. Soc. India **99**(2), 247–258 (2023d). https://doi.org/10.1007/s12594-023-2292-2

Ghosh, S., Saha, S., Bera, B.: Dynamics of total suspended solid concentrations in the lower Raidak river (Himalayan foreland Basin), India. Adv. Space Res. **71**(6), 2846–2861 (2023e). https://doi.org/10.1016/j.asr.2022.11.012

Ghosh, S., Sarkar, S., Bera, B.: Field based inventory of river bank erosion susceptibility model (BESI) of Raidak-II river in the Himalayan foreland basin. Phys. Geogr. **45**(2), 175–202 (2024). https://doi.org/10.1080/02723646.2023.2261180

Goswami, C., Mukhopadhyay, D., Poddar, B.C.: Tectonic control on the drainage system in a piedmont region in tectonically active eastern Himalayas. Front. Earth Sci. **6**, 29–38 (2012)

Hooke, J.M., Yorke, L.: Channel bar dynamics on multi-decadal timescales in an active meandering river. Earth Surf. Process. Landf. **36**(14), 1910–1928 (2011)

Howard, A.D.: Long profile development of bedrock channels: Interaction of weathering, mass wasting, bed erosion, and sediment transport. In: Geophysical Monograph-American Geophysical Union, vol. 107, pp. 297–319 (1998)

Leopold, L.B., Wolman, M.G.: River channel patterns: braided, meandering, and straight. US GPO (1957). https://doi.org/10.3133/pp282B

McFeeters, S.K.: The use of the Normalized Difference Water Index (NDWI) in the delineation of open water features. Int. J. Remote Sens. **17**(7), 1425–1432 (1996). https://doi.org/10.1080/01431169608948714

Miall, A.D.: A review of the braided-river depositional environment. Earth Sci. Rev. **13**(1), 1–62 (1977). https://doi.org/10.1016/0012-8252(77)90055-1

Miall, A.D.: Recent developments in the study of fluvial facies models (1987)

Micheli, E.R., Larsen, E.W.: River channel cutoff dynamics, Sacramento river, California, USA. River Res. Appl. **27**(3), 328–344 (2011)

Mueller, J.E.: An introduction to the hydraulic and topographic sinuosity indexes. Ann. Assoc. Am. Geogr. **58**(2), 371–385 (1968). https://doi.org/10.1111/j.1467-8306.1968.tb00650.x

Mueller, E.R., Pitlick, J.: Sediment supply and channel morphology in mountain river systems: 1. Relative importance of lithology, topography, and climate. J. Geophys. Res. Earth Surf. **118**(4), 2325–2342 (2013)

Nakata, T.: Geomorphic history and crustal movements of the foothills of the Himalayas (Doctoral dissertation, Tohoku University) (1972)

Nardi, L., Rinaldi, M.: Spatio-temporal patterns of channel changes in response to a major flood event: the case of the Magra River (central–northern Italy). Earth Surf. Process. Landf. **40**(3), 326–339 (2015)

Registrar General & Census Commissioner, India. Census of India 2011. Government of India, 2011. http://www.censusindia.gov.in/

Robert, A.: River Processes. Arnold, London (2003)

Robertson-Rintoul, M.S.E., Richards, K.S.: Braided-channel pattern and palaeohydrology using an index of total sinuosity. Geol. Soc. Spec. Publ. **75**(1), 113–118 (1993)

Rust, B.R.: Depositional models for braided alluvium (1977)

Saha, U.D., Saheb, A.M., Islam, A., Barman, S.D., Dutt, S., Islam, A.R.M.T.: Characterizing the trend of channel braiding of a tropical transboundary river using spatial growth component analysis and ARIMA model. Adv. Space Res. **70**(7), 1773–1794 (2022). https://doi.org/10.1016/j.asr.2022.06.032

Sarkar, S., Bera, B.: Around seven decades river course shifting and bank erosion susceptibility of river Mujnai. River **1**(2), 221–239 (2022). https://doi.org/10.1002/rvr2.19

Sarkar, S., Bera, B.: Reach scale channel planform dynamics of transboundary River Jaldhaka within Himalayan Foreland Basin. Phys. Geogr. (2024). https://doi.org/10.1080/02723646.2024.2356907

Sarkar, S., Roy, A., Bhattacharjee, S., Shit, P.K., Bera, B.: Effects of COVID-19 lockdown and unlock on health of

Bhutan-India-Bangladesh trans-boundary rivers. J. Hazard. Mater. **4**, 100030 (2021). https://doi.org/10.1016/j.hazadv.2021.100030
Sarkar, S., Bera, B., Bhattacharjee, S., Shit, P.K.: Large-scale stresses, decay of River Jamuna and resilience strategies in the Anthropocene. Quat. Sci. Adv. **12**, 100111 (2023). https://doi.org/10.1016/j.qsa.2023.100111
Schumm, S.A.: Sinuosity of alluvial rivers on the Great Plains. Geol. Soc. Am. Bull. **74**(9), 1089–1100 (1963)
Sharma, N.: Mathematical modelling and braid indicators. In: Singh, V.P. (ed.) The Brahmaputra River Basin Water Resources, vol. 47, pp. 229–260. Kluwer Academic Publishers, Dordrecht (2004)
Singh, A., Jaiswal, M.K., Pattanayak, J.K., et al.: Luminescence chronology of alluvial fan in North Bengal, India: implications to tectonics and climate. Geochronometria **43**, 102–112 (2016). https://doi.org/10.1515/geochr-2015-0037
Smith, N.D.: Sedimentology and bar formation in the upper Kicking Horse River, a braided outwash stream. J. Geol. **82**(2), 205–223 (1974). https://doi.org/10.1086/627959
Valdiya, K.S.: Dynamic Himalaya. Universities Press, Hyderabad (1998)
Xu, H.: Modification of normalised difference water index (NDWI) to enhance open water features in remotely sensed imagery. Int. J. Remote Sens. **27**(14), 3025–3033 (2006). https://doi.org/10.1080/01431160600589179
Yang, C.S., Ouchi, K.: Analysis of bar morphology using multi-temporal and multi-sensor satellite images: example from the Han Estuary, Korea. Mar. Geol. **311**, 17–31 (2012). https://doi.org/10.1016/j.margeo.2012.04.004
Zolezzi, G., Seminara, G.: Upstream influence in erodible beds. Phys. Chem. Earth B **26**(1), 65–70 (2001). https://doi.org/10.1016/S1464-1909(01)85016-4